Electronic Supplementary Material (ESI) for Biomaterials Science.

Supporting Information

Amphiphilic Mannose-6-Phosphate Glycopolypeptide-Based Bioactive and Responsive Self-Assembled Nanostructures for Controlled and Targeted Lysosomal Cargo Delivery

Basudeb Mondal,[a]# Bhawana Pandey,[b,c,d]# Nimisha Parekh,[b,c]# Sidharth Panda,[a] Tahiti Dutta,[a] Abinash Padhy[a] and Sayam Sen Gupta[a]*

Figure S6 The plot of fluorescence intensity versus the logarithm of the polymer concentration (μM) in aqueous solution (a) for $^{M6P}GP_{15}$-$^{A}PPO_{44}$ micelles (b) for $^{M6P}GP_{15}$-$(PCL_{25})_2$ micelles *Inset*: Fluorescence emission spectra of RBOE in an aqueous solution of a polymer at different concentrations.

Figure S7 Stability study of micelles (a) Time dependent hydrodynamic diameter of $^{M6P}GP_{15}$-$(PCL_{25})_2$ micelle over 20 days (b) Time dependent hydrodynamic diameter of $^{M6P}GP_{15}$-$^{A}PPO_{44}$ micelles over 20 days (c) Time dependent fluorescence intensity of RBOE loaded $^{M6P}GP_{15}$-$(PCL_{25})_2$ micelle (red) and $^{M6P}GP_{15}$-$^{A}PPO_{44}$ micelle (green).

Figure S8 MTT assay (metabolic activity) (a) for $^{M6P}GP_{15}$-$^{A}PPO_{44}$ block copolymer micelles and (b) for $^{M6P}GP_{15}$-$(PCL_{25})_2$ block polymer micelles, performed on MDA-MB-231 cell line.

Figure S9 MTT assay (metabolic activity) (a) for $^{M6P}GP_{15}$-$^{A}PPO_{44}$ block copolymer micelles and (b) for $^{M6P}GP_{15}$-$(PCL_{25})_2$ block polymer micelles, performed on MCF-7 cell line.

Figure S10. Colour intensity profile in MDA-MB-231 cells representing the variation of colour (both green and red) intensity with distance for a small sub-section of the merged image. MDA-MB-231 incubated with RBOE encapsulated $^{M6P}GP_{15}$-$^{A}PPO_{44}$ (a and d), $^{M6P}GP_{15}$-$(PCL_{25})_2$ micelles (b and e), and free RBOE (c and f) show only orange-yellowish spherical indicating co-localization of both dyes as is also observed object in the intensity profile.

Figure S11. Colour intensity profile in MCF-7 cells representing the variation of colour (both green and red) intensity with distance for a small sub-section of the merged image. MCF-7 incubated with RBOE encapsulated $^{M6P}GP_{15}$-$^{A}PPO_{44}$ (a and

d), $^{M6P}GP_{15}$-$(PCL_{25})_2$ micelles (b and e), and free RBOE (c and f) show only orange-yellowish spherical indicating co-localization of both dyes as is also observed object in the intensity profile.

Figure S12: Uptake of RBOE loaded $^{M6P}GP_{15}$-$^{A}PPO_{44}$ and $^{M6P}GP_{15}$-$(PCL_{25})_2$ onto MCF-7 and MDA-MB-231 cells: comparison of normalized fluorescence intensity analysis after cellular uptake of RBOE loaded $^{M6P}GP_{15}$-$^{A}PPO_{44}$ and $^{M6P}GP_{15}$-$(PCL_{25})_2$.

Figure S13. Competition assay for the uptake of RBOE loaded $^{M6P}GP_{15}$-$^{A}PPO_{44}$ and $^{M6P}GP_{15}$-$(PCL_{25})_2$ onto MDA-MB-231 cells: (a-c) fluorescence microscopy image of MDA-MB-231 cells treated with RBOE loaded $^{M6P}GP_{15}$-$^{A}PPO_{44}$; (d-f) fluorescence microscopy image of MDA-MB-231 cells that were first pretreated with 2.0 mM monomeric M6P followed by RBOE loaded $^{M6P}GP_{15}$-$^{A}PPO_{44}$ addition; (g-i)) fluorescence microscopy image of MDA-MB-231 cells treated with RBOE loaded $^{M6P}GP_{15}$-$(PCL_{25})_2$; and (j-l) fluorescence microscopy image of MDA-MB-231 cells that were first pretreated with 2.0 mM monomeric M6P followed by RBOE loaded $^{M6P}GP_{15}$-$(PCL_{25})_2$ addition.

Figure S14. Competition assay for the uptake of RBOE loaded $^{M6P}GP_{15}$-$^{A}PPO_{44}$ and $^{M6P}GP_{15}$-$(PCL_{25})_2$ onto MDA-MB-231 cells: normalized fluorescence intensity analysis after cellular uptake of RBOE loaded $^{M6P}GP_{15}$-$^{A}PPO_{44}$ and $^{M6P}GP_{15}$-$(PCL_{25})_2$ with and without monomeric M6P treatment.

Figure S15 MTT assay (metabolic activity) of Chlorpromazine performed on MDA-MB-231 cell line.

Figure S16 MTT assay (metabolic activity) of Genistein performed on MDA-MB-231 cell line.

Figure S17 MTT assay (metabolic activity) of Amiloride performed on MDA-MB-231 cell line.

Figure S18 Epifluorescence microscopy imaging of Calcein-Loaded $^{Man}GP_n$-$(PCL_n)_2$ vesicle (a, e and i); RBOE-Loaded $^{Man}GP_n$-$(PCL_n)_2$ vesicle (b, f and j); RBOE-Loaded $^{M6P}GP_{15}$-$(PCL_{25})_2$ micelle (c, g and k) and RBOE-Loaded $^{M6P}GP_{15}$-$^{A}PPO_{44}$ micelle (d, h and l).

Figure S19 Epifluorescence microscopy imaging and corresponding color intensity profile of RBOE-Loaded $^{Man}GP_n$-$(PCL_n)_2$ vesicle (a and d); RBOE-Loaded $^{M6P}GP_{15}$-$^{A}PPO_{44}$ micelle (b and e) and RBOE-Loaded $^{M6P}GP_{15}$-$(PCL_{25})_2$ micelle (c and f).

Figure S20 Histogram profile of RBOE-Loaded $^{Man}GP_n$-$(PCL_n)_2$ vesicle (a); RBOE-Loaded $^{M6P}GP_{15}$-$(PCL_{25})_2$ micelle (b) and RBOE-Loaded $^{M6P}GP_{15}$-$^{A}PPO_{44}$ micelle (c).

Figure S21 Epifluorescence microscopy imaging of FL-$^{M6P}GP_{15}$ polymer: Without any inhibitor (a, e, and i); Chlorpromazine treated (b, f, and j); Genistein treated (c, g, and k); Amiloride treated (d, h and l).

Figure S22 Epifluorescence microscopy imaging of RBOE-Loaded $^{M6P}GP_{15}$-ace-PPO_{44} micelle: Without any inhibitor (a, e, and i); Chlorpromazine treated (b, f, and j); Genistein treated (c, g, and k); Amiloride treated (d, h, and l).

Figure S23 Epifluorescence microscopy imaging of RBOE-Loaded $^{M6P}GP_{15}$-$(PCL_{25})_2$ micelle: Without any inhibitor (a, e, and i); Chlorpromazine treated (b, f, and j); Genistein treated (c, g, and k); Amiloride treated (d, h, and l).

Figure S24 Intensity of epifluorescence microscopy image of FL-$^{M6P}GP_{15}$, RBOE loaded $^{M6P}GP_{15}$-$^{A}PPO_{44}$ nanocarrier and RBOE loaded $^{M6P}GP_{15}$-$(PCL_{25})_2$ nanocarrier in the presence and absence of inhibitors chlorpromazine, amiloride and genistein.

Figure S25 ^{1}H NMR ($CDCl_3$, 200 MHz) Spectrum of Cl-$^{A}PPO_{44}$ polymer

Figure S26 ^{1}H NMR ($CDCl_3$**,** 200 MHz) Spectrum of N_3-$^{A}PPO_{44}$ polymer

Figure S27 ^{1}H NMR ($CDCl_3$, 200 MHz) Spectrum of N_3-$(PCL_{25})_2$ polymer

Figure S28 ^{1}H NMR ($CDCl_3$**,** 400 MHz) Spectrum of Pr-$^{M6P}AcGP_{15}$ polymer

Figure S29 ^{31}P NMR ($CDCl_3$, 202.46 MHz) Spectrum of Pr-$^{M6P}AcGP_{15}$

Figure S30 ^{1}H NMR ($CDCl_3$**,** 400 MHz) Spectrum of $^{M6P}AcGP_{15}$-$^{A}PPO_{44}$ block copolymer

Figure S31 ^{31}P NMR ($CDCl_3$, 202.46 MHz) Spectrum of $^{M6P}AcGP_{15}$-$^{A}PPO_{44}$ block copolymer

Figure S32 ^{1}H NMR (DMSO-d_6, 400 MHz) Spectrum of $^{M6P}GP_{15}$-$^{A}PPO_{44}$ block copolymer

Figure S33 ^{31}P NMR (DMSO-d_6, 202.46 MHz) Spectrum of $^{M6P}GP_{15}$-$^{A}PPO_{44}$ block copolymer

Figure S34 ^{1}H NMR ($CDCl_3$**,** 400 MHz) Spectrum of $^{M6P}AcGP_{15}$-$(PCL_{25})_2$ block copolymer

Figure S35 ^{31}P NMR ($CDCl_3$, 202.46 MHz) Spectrum of $^{M6P}AcGP_{15}$-$(PCL_{25})_2$ block copolymer

Figure S36 ^{1}H NMR (DMSO-d_6, 400 MHz) Spectrum of $^{M6P}AcGP_{15}$-$(PCL_{25})_2$ block copolymer

Figure S37 ^{31}P NMR (DMSO-d_6, 202.46 MHz) Spectrum of $^{M6P}AcGP_{15}$-$(PCL_{25})_2$ block copolymer

General Experimental Techniques and Apparatus

Instrumentation:

FT-IR spectra were recorded on a PerkinElmer FT-IR spectrum GX instrument by making KBr pellets. Pellets were prepared by mixing 3.0 mg of the sample with 97.0 mg of KBr. ^{1}H NMR spectra were recorded on Bruker Spectrometers (200, 400, or 500 MHz). ^{13}CNMR spectra were recorded on Bruker Spectrometer (50, 100 or 125 MHz) and reported relative signals according to the deuterated solvent used. ^{31}P NMR spectra recorded on Bruker Spectrometer (202.46 MHz) using an internal 85% aqueous H_3PO_4 as a reference. Gel permeation chromatography/light scattering (GPC/LS) was performed on a VISKOTEK TDA 305-040 TRIPLE DETECTOR ARRAY GPC/SEC MODULE. Separations were achieved by three columns (T6000M, GENERAL MIXED ORG 300X7.8 MM) and one guard column (TGAURD, ORG GUARD COL 10X4.6 MM), 0.05 M LiBr in DMF as the eluent at 60°C. GPC/LS samples were prepared at concentrations of 5 mg/mL. A constant flow rate of 1 mL/min was maintained. The system was calibrated by PMMA standards. CD (190−250 nm) spectra of the polypeptides (1.0−0.25 mg/mL in water or buffer) were recorded by JASCO J-815 CD spectrophotometer in a cuvette with 1 mm path length. All the spectra were recorded for an average of three scans, and the spectra were reported as a function of molar ellipticity [θ] versus wavelength. The molar ellipticity was calculated using the standard formula, $[\theta]=(\theta \times 100 \times Mw)/(C \times l)$, where θ = experimental ellipticity in millidegrees, Mw and C was molecular weight and concentration of the amino acid repeat unit, and l = path length in cm. The % α helicity was calculated by using the formula: % α helicity = $[(-[\theta]_{222}\ nm + 3000)/39000] \times 100$. Hydrodynamic size distribution mesurements were performed on Malvern Zetasizer

instrument. All data were recorded for an average of three scans, and the data were reported as a function of intensity versus diameter (d, nm). Transmission electron microscopy (TEM) measurements were performed at 200 kV on a FEI Technai F20 and F30 instrument. Atomic force microscopy (AFM) analysis was performed on the Asylum Research, USA, MFP-3D BIO instrument (Operating Mode: Contact mode AFM under dry and wet conditions; System Specification: Closed loop sensors on all three axes : X & Y range 90 µm, X & Y sensors <0.5 nm noise, <0.5% non-linearity; Z range >15 µm, Z sensor <0.25 nm noise; Optional Extended Z Head with range >40 µm; DC height noise <50 pm). Fluorescence experiments were carried out on fluorimeter QM40 from Photon Technology International.

Materials and methods

Other chemicals and solvents such as petroleum ether, ethyl acetate, diethyl ether, tetrahydrofuran, dioxane and dichloromethane were obtained from Merck, India. They are dried by using conventional drying methods and finally stored in glove-box prior to use. Unless otherwise reported, all reactions were performed under argon atmosphere. Removal of solvent *in vacuum* using a rotary evaporator attached to an efficient vacuum pump and products obtained as solids or syrups were dried under high vacuum. Analytical thin-layer chromatography was performed on pre-coated silica plates (F254, 0.25 mm thickness); compounds were visualized by UV light or by staining with anisaldehyde spray.

General procedure for synthesis of azide-containing poly(propylene glycol): N_3-$^{A}PPO_{44}$

(1) **Synthesis of acetal containing chloro-terminated poly(propylene glycol) monobutyl ether: Cl-^{A}PPO$_{44}$**

Polypropylene glycol monobutyl ether (M_n = 2500 g/mol) (5 g, 2.0 mmol) and pyridine p-toluene sulphonate (PPTS) (0.125 g, 0.49 mmol) were dried by azeotropic distillation with toluene just before start of the reaction. The reaction mixture was then dissolved in 50 mL dry DCM and chloroethyl vinyl ether (CEVE) (2.12 g, 20 mmol) was added by dissolving in 10 mL dry DCM dropwise over 15 min under an argon atmosphere at 0 °C. After 1 hr, 20 mL of 5 wt% Na_2CO_3 solution was added to quench the reaction and to avoid the cleavage of the acetal linkage. The reaction mixture was then diluted with 100 mL DCM and washed with brine solution. Finally, the reaction mixture was precipitated into cold hexane and the product was dried under vacuum. (Yield: 4.46 g, 85%)

^{1}H NMR (200MHz, $CDCl_3$): δ (ppm) 1.10-1.31 (d, 130H), 3.36-3.56 (m, 131H), 4.80 (q, 1H).

(2) Synthesis of acetal containing azide terminated poly(propylene glycol) monobutyl ether: N_3-^{A}PPO$_{44}$

Cl-^{A}PPO$_{44}$ (5 g, 2.0 mmol), NaN_3 (1.3 g, 20 mmol) was dissolved in DMF and stirred at 60 °C for 24 hr. After completion of the reaction, DMF was removed under reduced pressure. The crude product was precipitated in cold diethyl ether and the obtained white product was dried under vacuum. (Yield: 4.2 g, 83%)

^{1}H NMR (200MHz, $CDCl_3$): δ (ppm) 1.10-1.31(d, 130H), 3.36-3.56 (m, 131H), 4.79 (q, 1H).

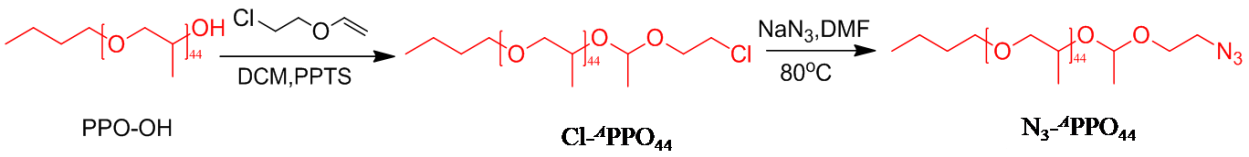

Scheme S1: Synthesis of acetal containing azide terminated poly (propylene glycol) monobutyl ether (N_3-$^{A}PPO_{44}$) as acid-cleavable hydrophobic block.

General procedure for synthesis of azide-containing polycaprolactone: N_3-$(PCL_{25})_2$

(1) Synthesis of Difunctional ROP-Initiator: (2, 2'-((2-azidoethyl) azanediyl) diethanol)

Chloroethanol was converted to azidoethanol using NaN_3 in the water at reflux condition for 12 hr, which after reaction with p-toluenesulfonic acid in DCM at room temperature gives 2-azidoethyl p-toluenesulfonate. Into a 250 mL two-necked round-bottom flask equipped with a dropping funnel were charged, 2, 2'azanediyldiethanol (20.91 g, 199 mmol), and dry THF (70 mL). The reaction mixture was stirred for 15 minutes. The solution of 2-azidoethyl p-toluenesulfonate (12 g, 10 mmol) in THF (50 mL) was added drop wise under constant stirring at room temperature. The reaction mixture was heated at 80 °C for 8 hr. The reaction mixture was cooled to room temperature. Residue obtained after removal of THF was dissolved in water (100 mL) and then extracted with dichloromethane (500 mL). The organic layer was dried over anhydrous sodium sulfate, filtered, and chloroform was evaporated under reduced pressure. The crude product was purified by silica gel column chromatography using a mixture of (ethyl acetate: pet ether: methanol (30:70:2.5, v/v) as eluent. The removal of the solvent afforded the product as a light brown liquid. (Yield: 5.2 g, 60 %)

^{1}H NMR (200MHz, $CDCl_3$): δ (ppm) 2.65-2.82 (6H, -N-C**H**$_2$CH$_2$-), 3.05 (2H, -CH$_2$O**H**), 3.40 (2H, N_3-C**H**$_2$CH$_2$-), 3.63 (4H, -C**H**$_2$-OH).

(2) Polymerization reaction

A Schlenk tube was charged with the initiator, ε-caprolactone, and stannous (II) octanoate under the nitrogen atmosphere. The reaction mixture was degassed three times by freeze pump thaw cycles. Polymerization was carried out under vacuum at 110 °C. When the solution became viscous viscous, the polymerization was terminated by cooling to room temperature and by releasing the vacuum to introduce air. Dichloromethane was added, and the resulting solution was precipitated in methanol, and the residue was filtered and dried in vacuum for 24 hr to obtain white powder.

***Branched polymer $(PCL_{25})_2$*:**

From difunctional initiator 2,2'-((2-azidoethyl) azanediyl) di-ethanol (0.574 mmol), ε-caprolactone (34.44 mmol) and stannous (II) octanoate (0.086 mmol). (Yield 82%).

^{1}H NMR (200MHz, $CDCl_3$): δ (ppm) 1.42 (104H, -COCH$_2$CH$_2$C**H**$_2$CH$_2$CH2O-), 1.64 (214H, -COCH$_2$C**H**$_2$CH$_2$C**H**$_2$CH$_2$O-), 2.34 (108H, -COC**H**$_2$CH$_2$CH$_2$CH$_2$CH$_2$O-), 2.68-2.86 (6H, -N-C**H**$_2$CH$_2$-), 3.26 (2H, N_3-C**H**$_2$CH$_2$-), 3.67 (4H, -C**H**$_2$-OH), 4.06 (105H, -COCH$_2$CH$_2$CH$_2$CH$_2$C**H**$_2$O-).

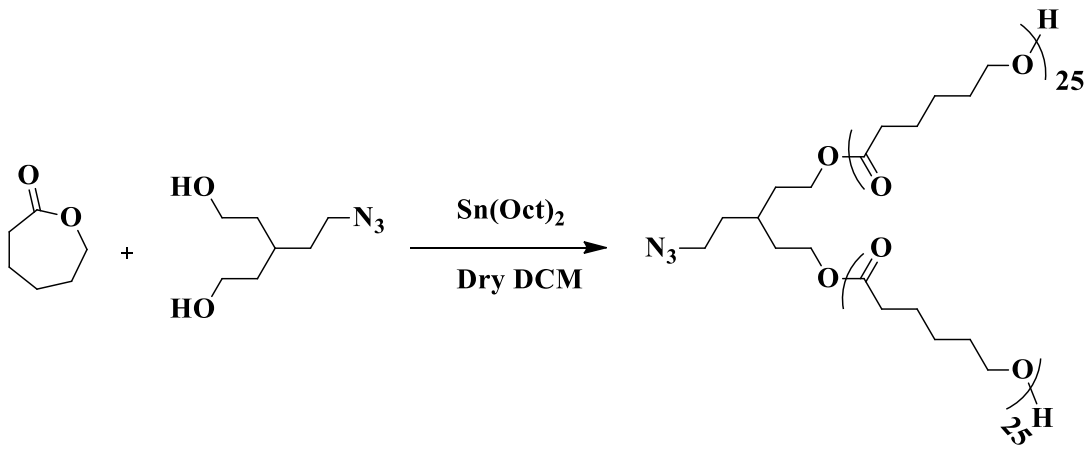

Scheme S2: Synthesis of azide-containing polycaprolactone N_3-$(PCL_{25})_2$ as a hydrophobic block.

General Procedure for the Synthesis of M6P-Glycopolypeptides: Pr-^{M6P}AcGP$_{15}$

(1) Preparation of N-Carboxyanhydride of 6-dibenzyl phosphate-2,3,4-tri-O-acetyl-β-D-mannopyranoside-L-lysine derivative: (M6P-NCA)

To a solution of 6-dibenzyl phosphate-2,3,4-tri-O-acetyl-β-D-mannopyranoside-L-lysine derivative (0.1 mmol) in freshly distilled anhydrous tetrahydrofuran (30 mL) was added a solution of triphosgene (0.05 mmol) in anhydrous tetrahydrofuran (5 mL) under argon atmosphere. N-methylmorpholine (0.1 mmol) was then added, and the reaction mixture was heated to 50 °C for 1.5 hr and cooled to room temperature following which the solids were removed using a glass fritted funnel. The clear solution was added to dry hexane with stirring, and the formation of a white precipitate was observed. The white solids were vacuum filtered using another glass frit funnel and re-dissolved in dry ethyl acetate purification using anhydrous column chromatography. The column was packed with vacuum-dried silica (60-100 mesh) in dry hexane. The crude product was purified with a gradient of freshly distilled 1:3 hexane/EtOAc through the column and then 1% dry

acetone in EtOAc as the eluent. The fraction containing the desired product was dried under vacuum to yield a white fluffy solid NCA (Yield 58%).

^{1}H NMR (399.78 MHz, $CDCl_3$): δ(ppm) 1.46-1.60 (m, 5H), 2.01-2.10 (m, 10H), 3.29-3.38 (m, 2H), 3.93-4.27 (m, 6H), 4.82 (s, 1H), 5.02-5.06 (m, 4H), 5.23-5.36 (m, 3H), 6.65-6.71 (t, 1H), 7.34 (m, 10H), 7.92 (s, 1H).

^{13}C NMR (100 MHz, $CDCl_3$): δ(ppm) 20.59, 20.68, 22.16, 28.50, 31.33, 38.22, 57.51, 65.56, 65.89, 66.01, 66.81, 68.80, 69.04, 69.54, 69.66, 97.25, 126.92, 127.89-128.59 (10C), 135.39, 135.53, 152.16, 168.20, 169.67, 170.36, 170.41, 170.66.

^{31}P NMR (202.46 MHz, $CDCl_3$): δ(ppm) -1.38.

(2) Synthesis of alkyne functionalized M6P-glycopolypeptides: Pr-^{M6P}AcGP$_{15}$

To a solution of M6P-NCA (100 mg/mL) in dry DMF was added with “proton sponge” N,N´-tetramethylnapthalene (0.5 equiv to monomer; 1 M) as an additive and propargylamine (0.5 M) as the initiator inside the glove box. The progress of the polymerization was monitored by FT-IR spectroscopy by comparing it with the intensity of the initial NCAs anhydride stretching at 1784 cm^{-1} and 1854 cm^{-1}. The polymerization reactions were generally complete within 36 hr. Aliquots were removed after completion of polymerization for GPC analysis. Finally, the solvent was removed under reduced pressure from the reaction mixture. The resulting residue was re-dissolved in dichloromethane, and then the polymer was precipitated out by the addition of diethyl ether. The precipitated polymer was collected by centrifugation and dried to afford white M6P-glycopolypeptides in almost 90-95% yield.

^{1}H NMR (399.78 MHz, $CDCl_3$): δ(ppm) 0.85 (3H), 1.28-1.57 (5H), 1.95-2.13 (10H), 3.22-3.38 (2H), 3.98-4.12 (6H), 4.83-4.86 (1H), 5.05 (4H), 5.33 (3H), 6.71, 7.38 (10H), 7.78.

^{31}P NMR (202.46 MHz, $CDCl_3$): δ(ppm) -1.29

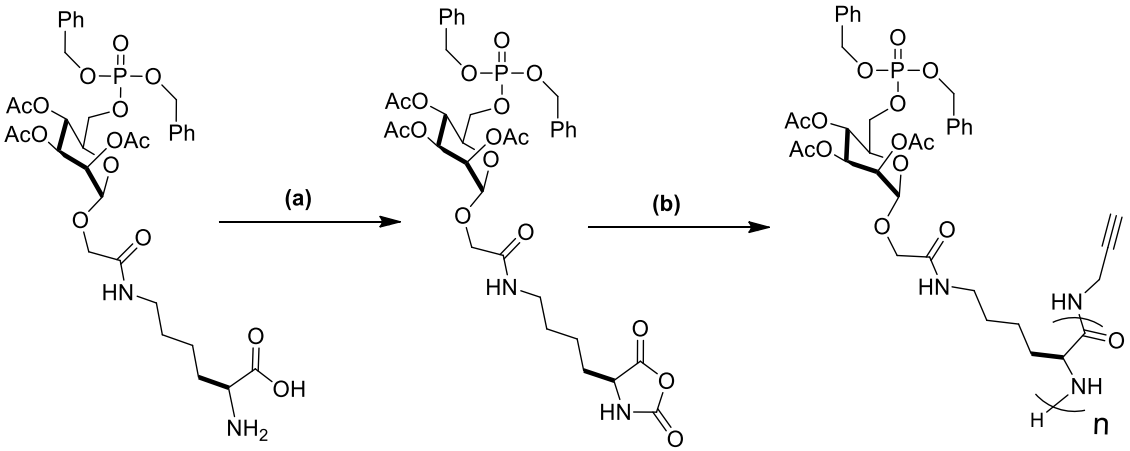

(a) Triphosgene, N-methyl morpholine, THF, 55 °C, 1 hr (58% yield); (b) propargylamine, proton sponge, DMF (~95% yield)

Scheme S3: Synthesis of alkyne functionalized M6P-glycopolypeptides (Pr-^{M6P}AcGP_{15}).

Sample preparation for TEM, AFM and DLS analysis:

On a carbon-coated 400 mesh copper grid about 10 µL of 0.1 wt% solution of the deprotected block copolymer was spotted and kept for 15-20 min, the excess solvent was removed by shocking of solvent with Whatman filter paper. Then the grid was negatively stained by 0.2 wt% uranyl acetate for 3-4 s, and excess solvent was removed. The grid was washed thrice with deionized water to remove excess unbound uranyl acetate from the grid. Grids were dried in a desiccator for 20 hr and analyzed by transmission electron microscopy. For AFM analysis, aqueous solution (0.02 wt%) was dropped cast on a silicon wafer and then dried for 24 hr. An aqueous solution (0.1 wt%) of the block

copolymer was filtered using 0.45 μm filter, and hydrodynamic diameter was determined by dynamic light scattering (DLS) analysis.

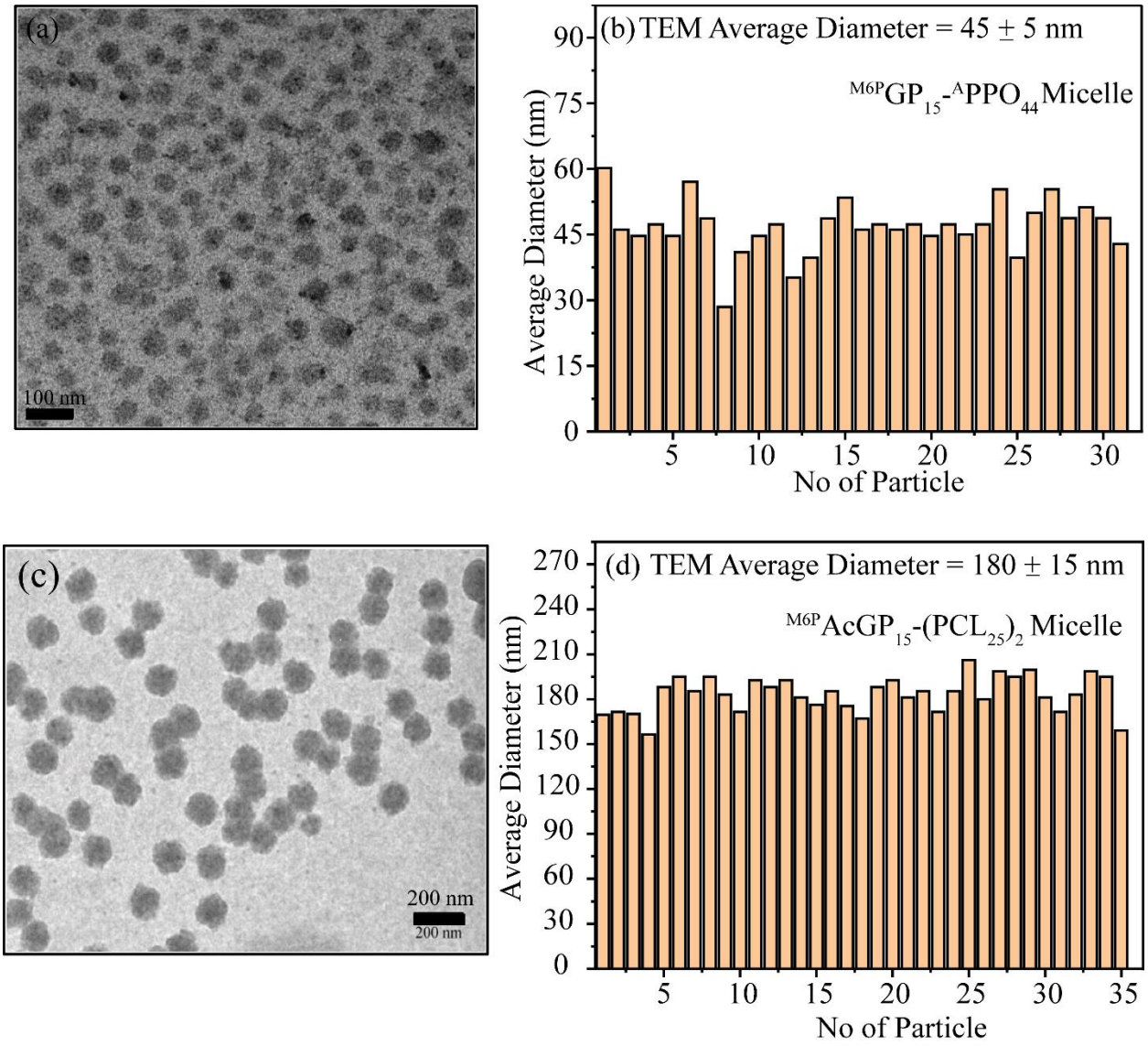

Figure S1 TEM analysis of $^{M6P}GP_{15}$-$^{A}PPO_{44}$ (a and b) micelles and the $^{M6P}GP_{15}$-$(PCL_{25})_2$ (c and d) micelles

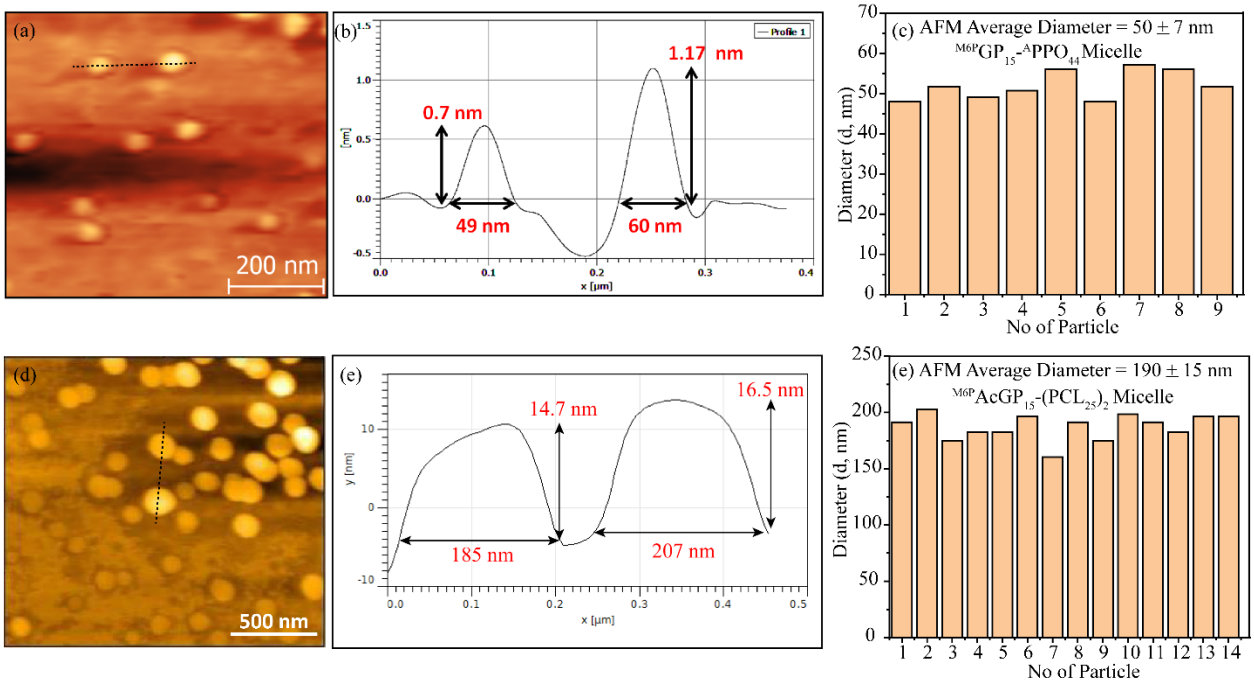

Figure S2 AFM line profile and average diameter of $^{M6P}GP_{15}$-$^{A}PPO_{44}$ (a, b, and c) micelles and the $^{M6P}GP_{15}$-$(PCL_{25})_2$ (d, e, and f) micelles

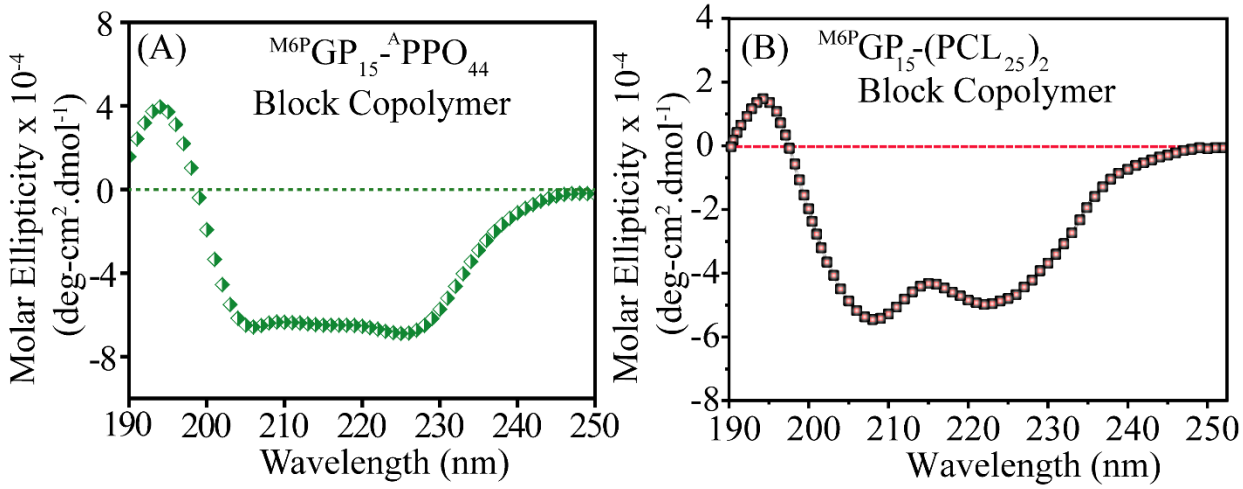

Figure S3 CD spectrum of (A) $^{M6P}GP_{15}$-$^{A}PPO_{44}$ and (B) $^{M6P}GP_{15}$-$(PCL_{25})_2$ block copolymers.

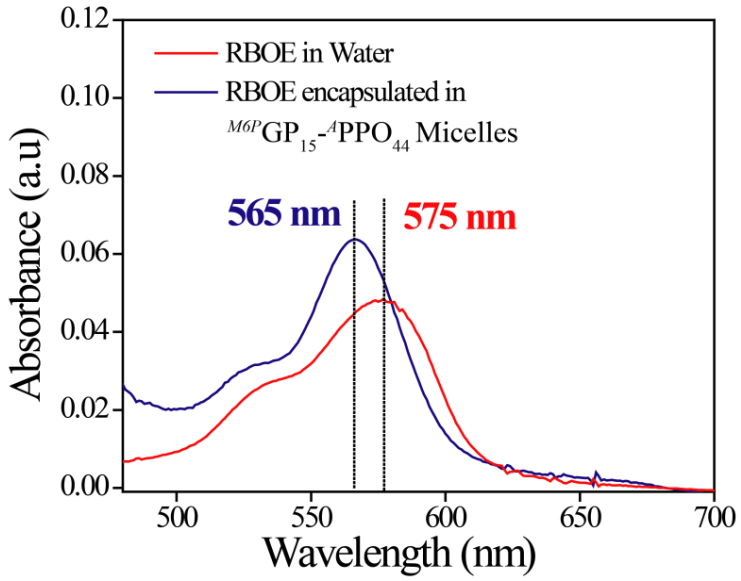

Figure S4 UV-Vis absorption spectra of free RBOE in water and RBOE encapsulated in $^{M6P}GP_{15}$-$^{A}PPO_{44}$ micelles**.**

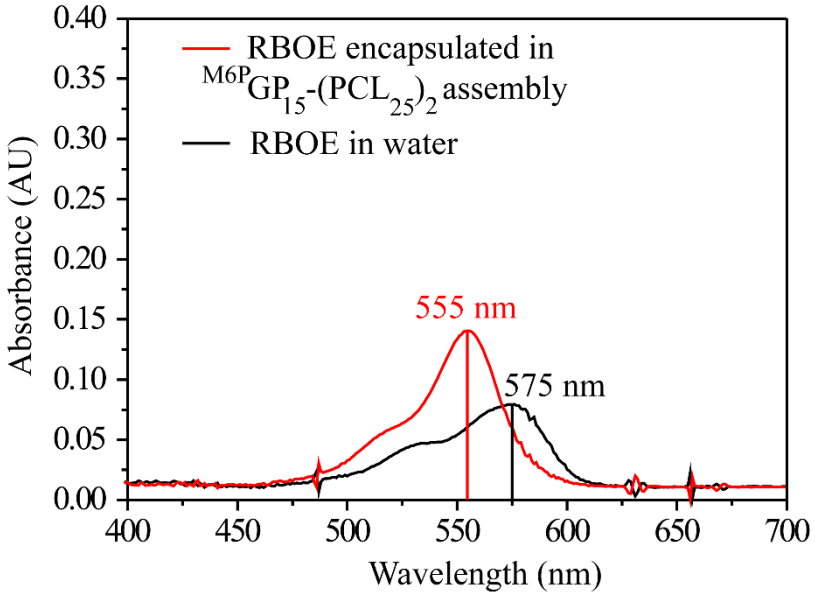

Figure S5 UV-Vis absorption spectra of free RBOE in water and RBOE encapsulated in $^{M6P}GP_{15}$-$(PCL_{25})_2$ micelles

Critical micelle concentration determination of $^{M6P}GP_{15}$-$^{A}PPO_{44}$ and $^{M6P}GP_{15}$-$(PCL_{25})_2$ Micellar system.

(1) For $^{M6P}GP_{15}$-$^{A}PPO_{44}$ system:

Critical micelle concentration (CMC) of micelles is determined by fluorescence spectroscopy using rhodamine B octadecyl ester (RBOE) as a hydrophobic fluorescence probe. The final stock solution of prepared micelles (142.9 µM) was serially diluted and concentration was varied from 1 mg/mL to 4.88 x 10^{-4} mg/mL. The serially diluted micellar solutions were mixed with RBOE in acetone to make a final concentration of RBOE of 1.25 µM. The solutions are allowed to stir overnight. Then the emission spectra were recorded with the excitation wavelength at 560 nm. The fluorescence intensity of RBOE at 580 nm was plotted against the concentration of micelles.

(**2) For $^{M6P}GP_{15}$-$(PCL_{25})_2$ system:**

Critical micelle concentration (CMC) of micelles is determined by fluorescence spectroscopy using rhodamine B octadecyl ester (RBOE) as a hydrophobic fluorescence probe. The final stock solution of prepared micelles (27.77 µM) was serially diluted, and concentration was varied from 0.5 mg/mL to 1.95 x 10^{-3} mg/mL. The serially diluted micellar solutions were mixed with RBOE in acetone to make a final concentration of RBOE of 1.25 µM. The solutions are allowed to stir overnight. Then the emission spectra were recorded with the excitation wavelength at 560 nm. The fluorescence intensity of RBOE at 580 nm was plotted against the concentration of micelles.

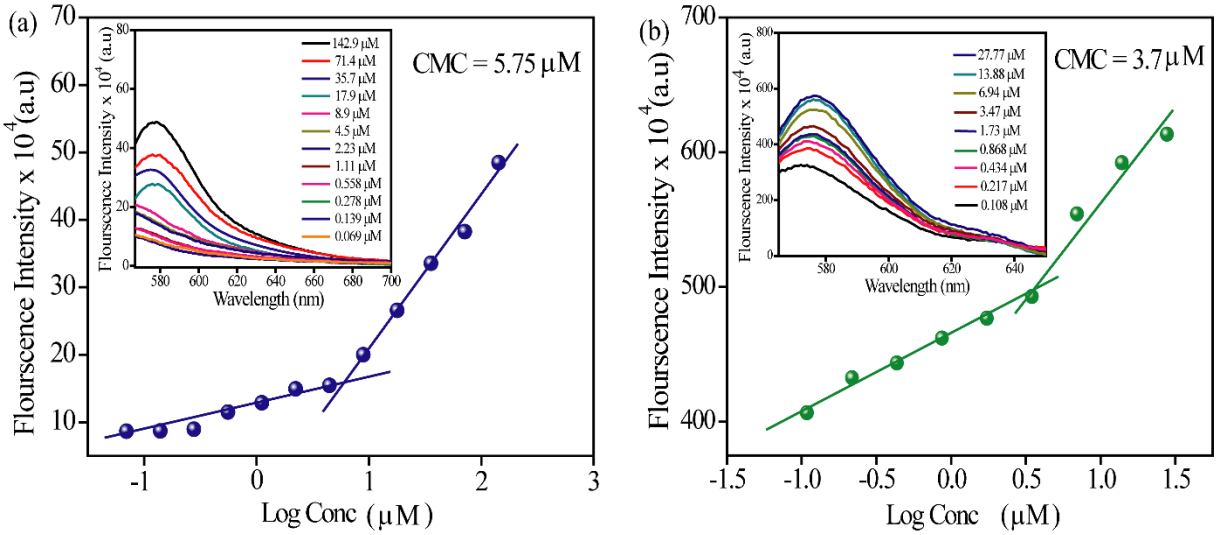

Figure S6 The plot of fluorescence intensity versus the logarithm of the polymer concentration (μM) in aqueous solution (a) for $^{M6P}GP_{15}$-$^{A}PPO_{44}$ micelles (b) for $^{M6P}GP_{15}$-$(PCL_{25})_2$ micelles *Inset*: Fluorescence emission spectra of RBOE in an aqueous solution of a polymer at different concentrations.

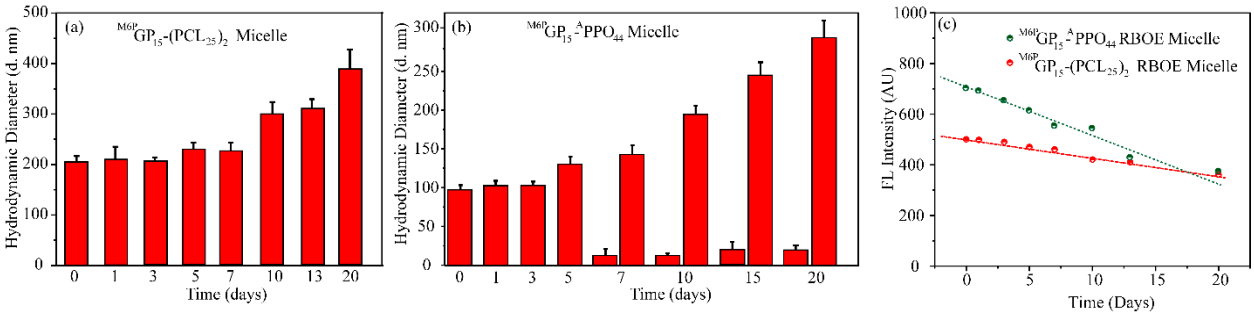

Figure S7 Stability study of micelles (a) Time dependent hydrodynamic diameter of $^{M6P}GP_{15}$-$(PCL_{25})_2$ micelle over 20 days (b) Time dependent hydrodynamic diameter of $^{M6P}GP_{15}$-$^{A}PPO_{44}$ micelles over 20 days (c) Time dependent fluorescence intensity of RBOE loaded $^{M6P}GP_{15}$-$(PCL_{25})_2$ micelle (red) and $^{M6P}GP_{15}$-$^{A}PPO_{44}$ micelle (green).

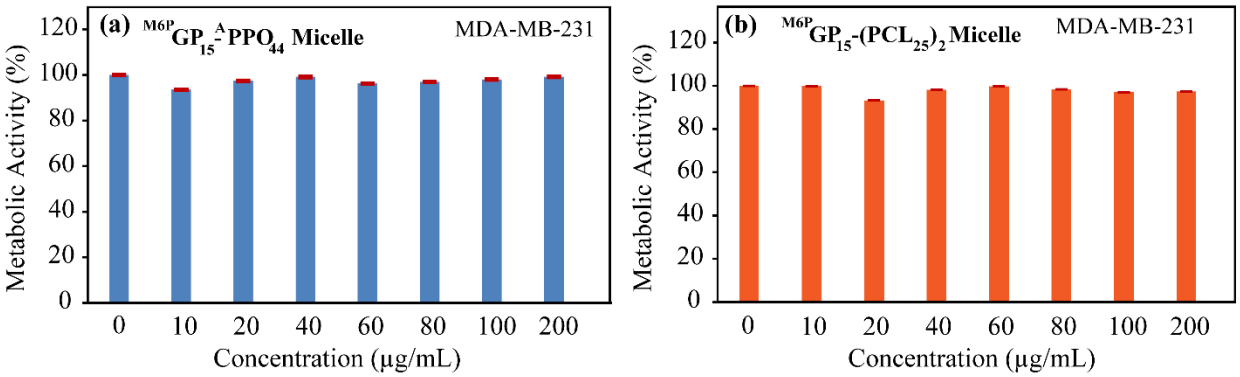

Figure S8 MTT assay (metabolic activity) (a) for $^{M6P}GP_{15}$-$^{A}PPO_{44}$ block copolymer micelles and (b) for $^{M6P}GP_{15}$-$(PCL_{25})_2$ block polymer micelles, performed on MDA-MB-231 cell line.

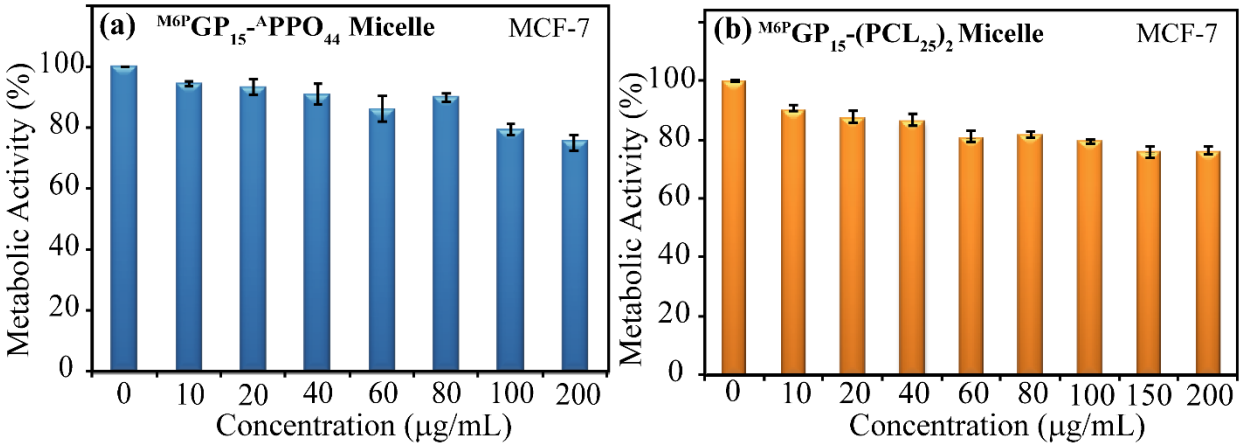

Figure S9 MTT assay (metabolic activity) (a) for $^{M6P}GP_{15}$-$^{A}PPO_{44}$ block copolymer micelles and (b) for $^{M6P}GP_{15}$-$(PCL_{25})_2$ block polymer micelles, performed on MCF-7 cell line.

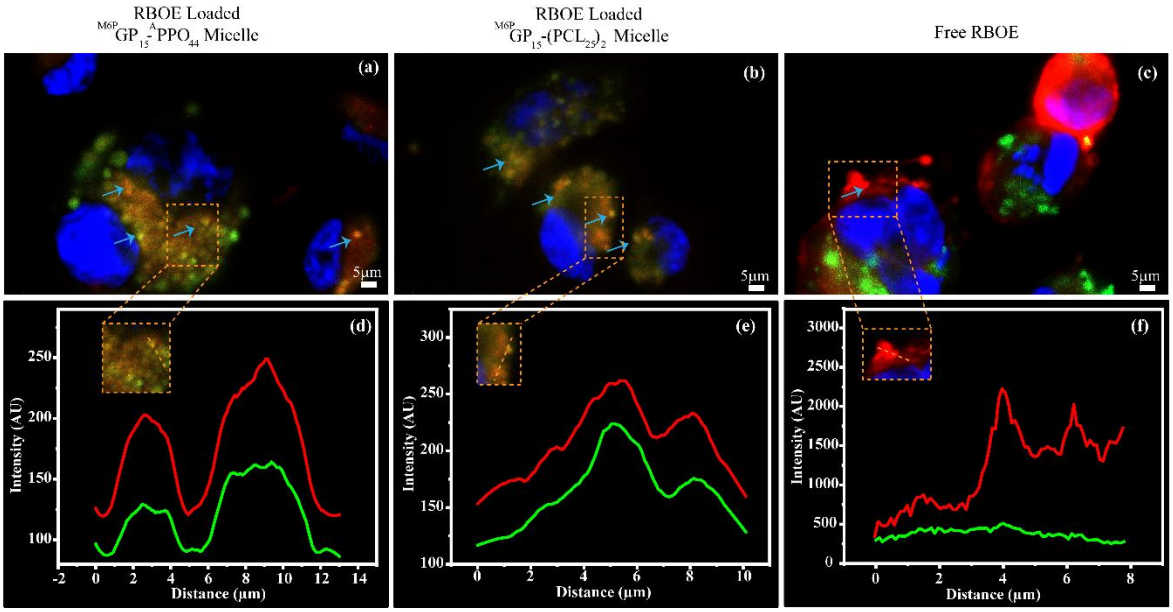

Figure S10. Colour intensity profile in MDA-MB-231 cells representing the variation of colour (both green and red) intensity with distance for a small sub-section of the merged image. MDA-MB-231 incubated with RBOE encapsulated $^{M6P}GP_{15}$-$^{A}PPO_{44}$ (a and d), $^{M6P}GP_{15}$-$(PCL_{25})_2$ micelles (b and e), and free RBOE (c and f) show only orange-yellowish spherical indicating co-localization of both dyes as is also observed object in the intensity profile.

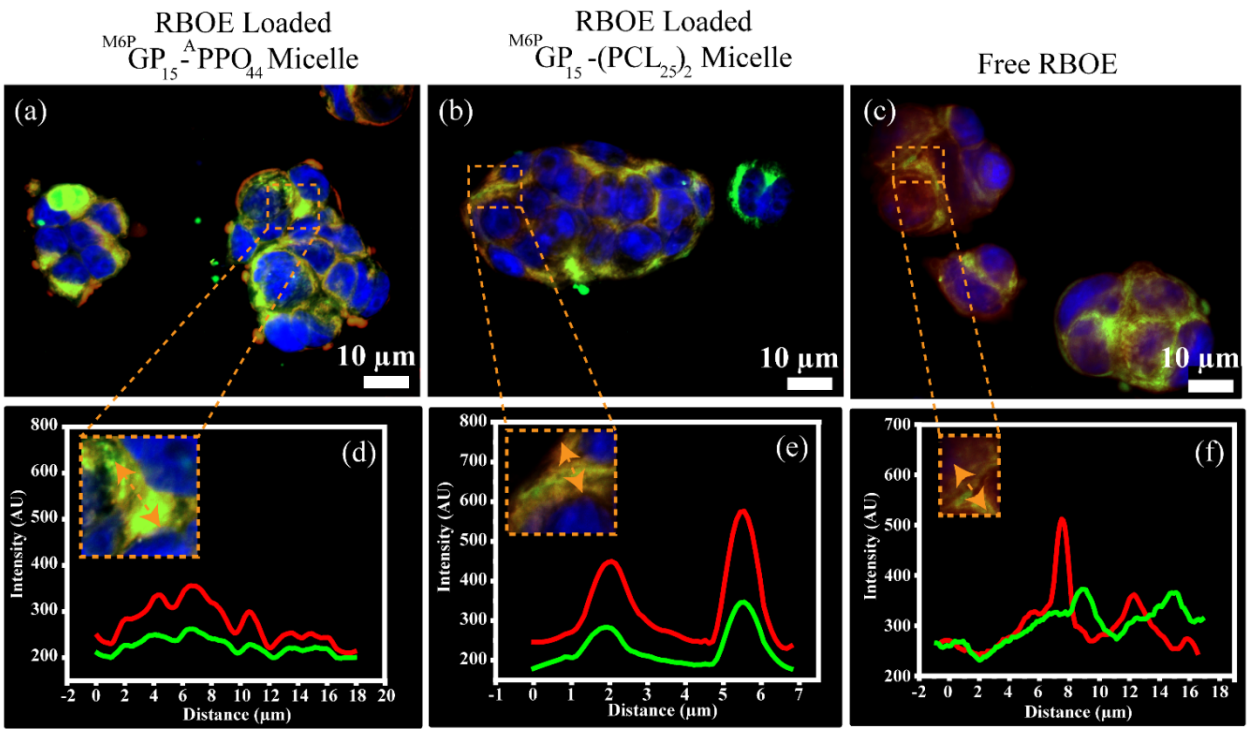

Figure S11. Colour intensity profile in MCF-7 cells representing the variation of colour (both green and red) intensity with distance for a small sub-section of the merged image. MCF-7 incubated with RBOE encapsulated $^{M6P}GP_{15}$-$^{A}PPO_{44}$ (a and d), $^{M6P}GP_{15}$-$(PCL_{25})_2$ micelles (b and e), and free RBOE (c and f) show only orange-yellowish spherical indicating co-localization of both dyes as is also observed object in the intensity profile.

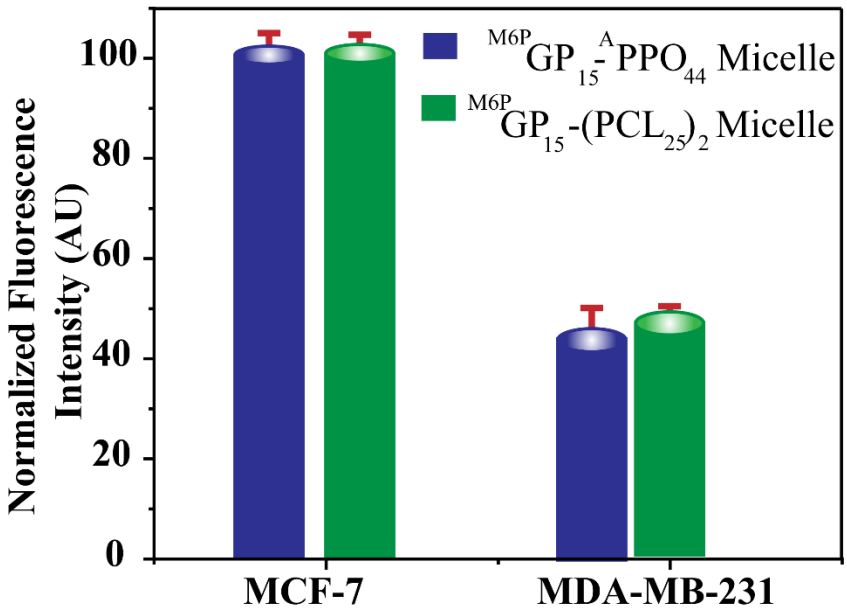

Figure S12: Uptake of RBOE loaded $^{M6P}GP_{15}$-$^{A}PPO_{44}$ and $^{M6P}GP_{15}$-$(PCL_{25})_2$ onto MCF-7 and MDA-MB-231 cells: comparison of normalized fluorescence intensity analysis after cellular uptake of RBOE loaded $^{M6P}GP_{15}$-$^{A}PPO_{44}$ and $^{M6P}GP_{15}$-$(PCL_{25})_2$.

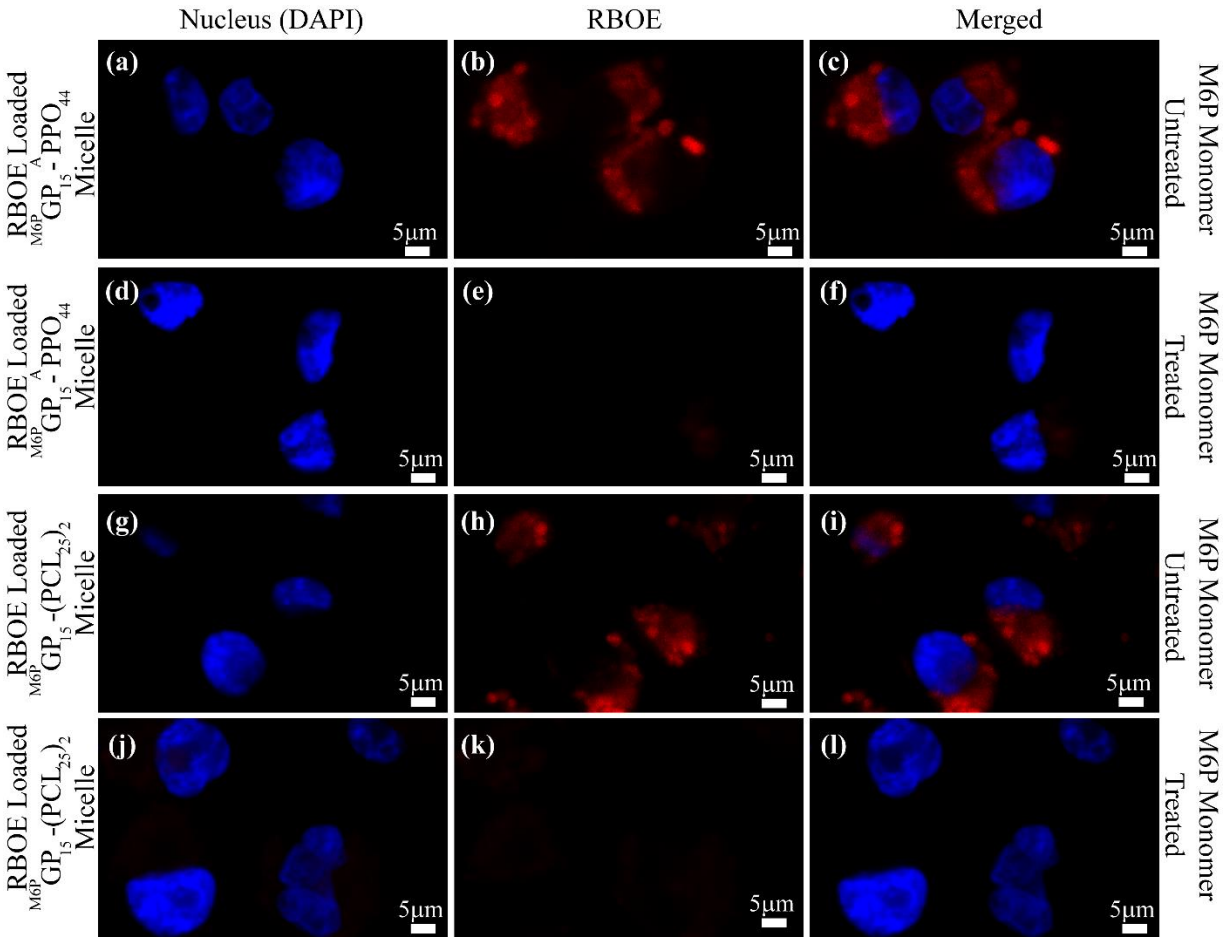

Figure S13. Competition assay for the uptake of RBOE loaded $^{M6P}GP_{15}$-$^{A}PPO_{44}$ and $^{M6P}GP_{15}$-$(PCL_{25})_2$ onto MDA-MB-231 cells: (a-c) fluorescence microscopy image of MDA-MB-231 cells treated with RBOE loaded $^{M6P}GP_{15}$-$^{A}PPO_{44}$; (d-f) fluorescence microscopy image of MDA-MB-231 cells that were first pretreated with 2.0 mM monomeric M6P followed by RBOE loaded $^{M6P}GP_{15}$-$^{A}PPO_{44}$ addition; (g-i)) fluorescence microscopy image of MDA-MB-231 cells treated with RBOE loaded $^{M6P}GP_{15}$-$(PCL_{25})_2$; and (j-l) fluorescence microscopy image of MDA-MB-231 cells that were first pretreated with 2.0 mM monomeric M6P followed by RBOE loaded $^{M6P}GP_{15}$-$(PCL_{25})_2$ addition.

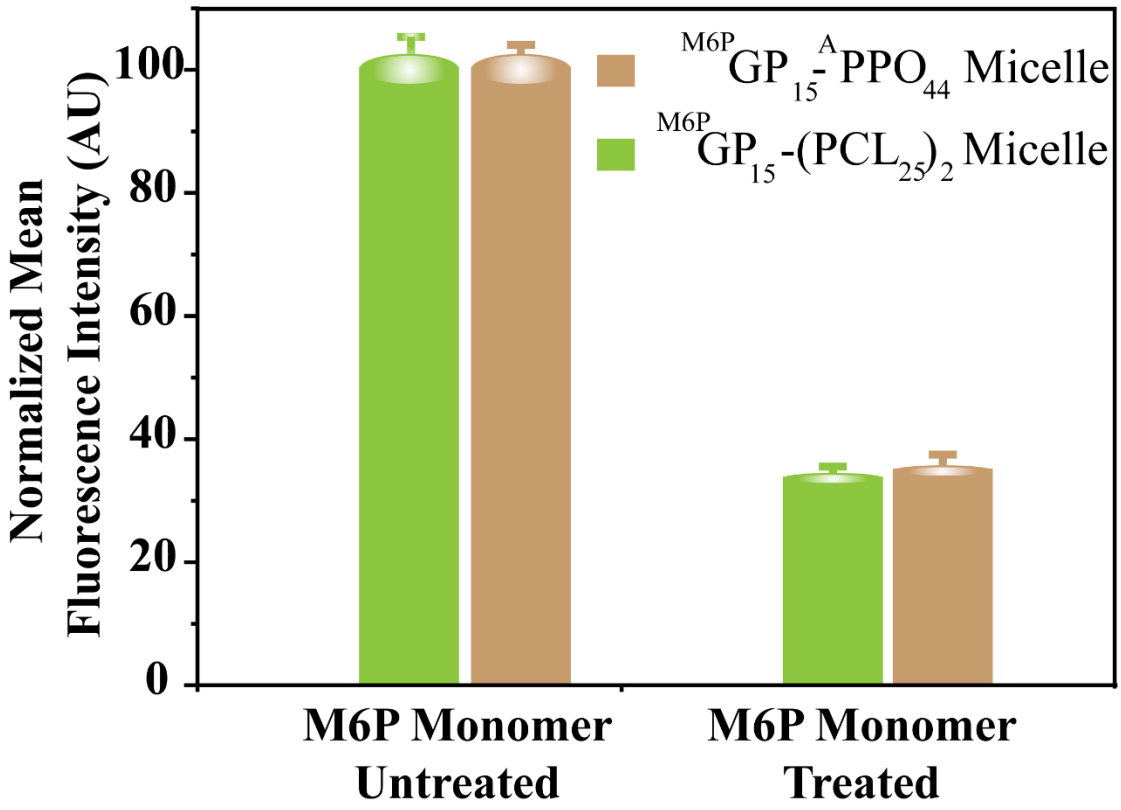

Figure S14. Competition assay for the uptake of RBOE loaded $^{M6P}GP_{15}$-$^{A}PPO_{44}$ and $^{M6P}GP_{15}$-$(PCL_{25})_2$ onto MDA-MB-231 cells: normalized fluorescence intensity analysis after cellular uptake of RBOE loaded $^{M6P}GP_{15}$-$^{A}PPO_{44}$ and $^{M6P}GP_{15}$-$(PCL_{25})_2$ with and without monomeric M6P treatment.

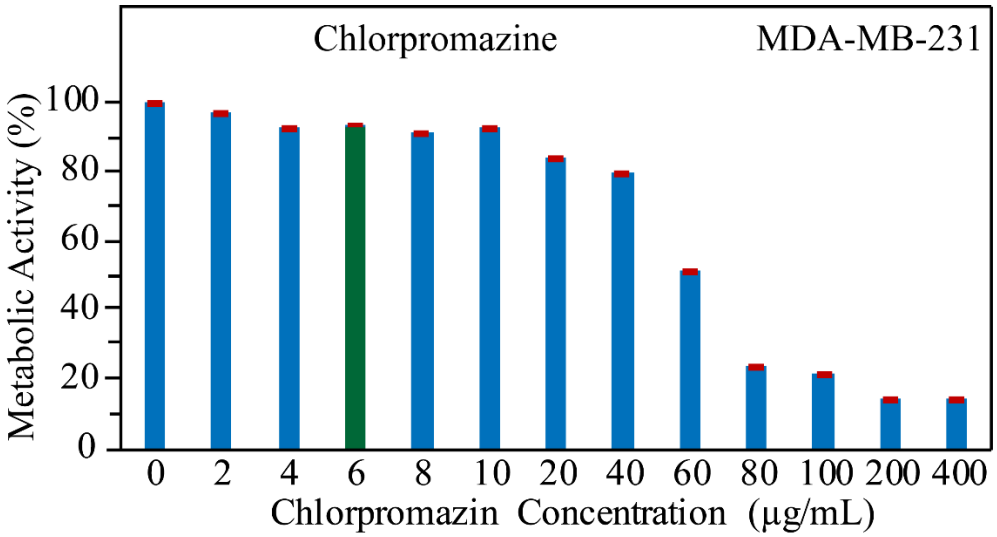

Figure S15 MTT assay (metabolic activity) of Chlorpromazine performed on MDA-MB-231 cell line.

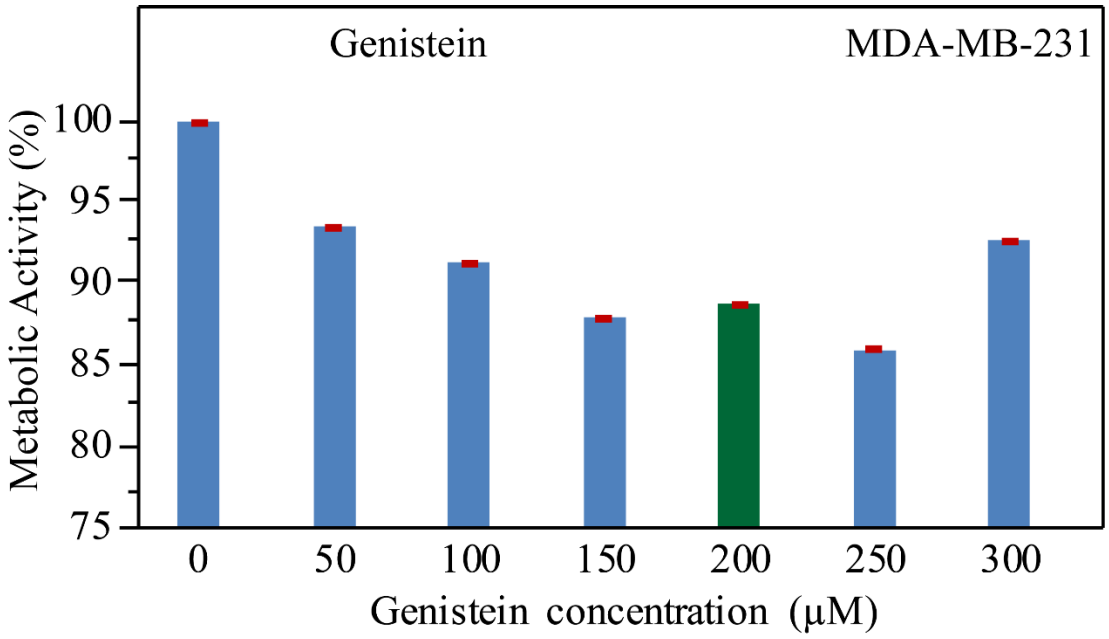

Figure S16 MTT assay (metabolic activity) of Genistein performed on MDA-MB-231 cell line.

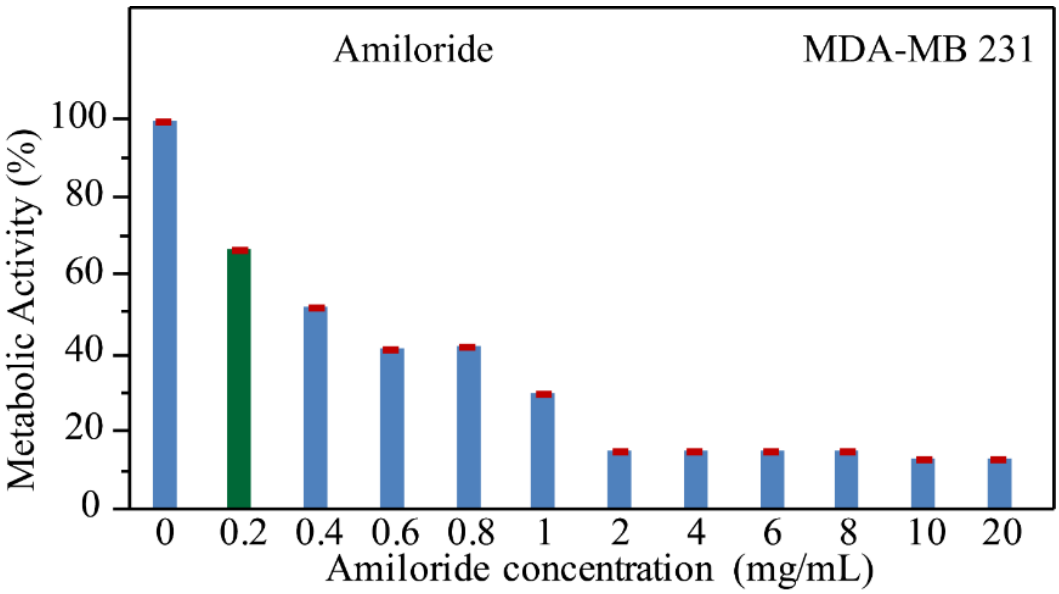

Figure S17 MTT assay (metabolic activity) of Amiloride performed on MDA-MB-231 cell line.

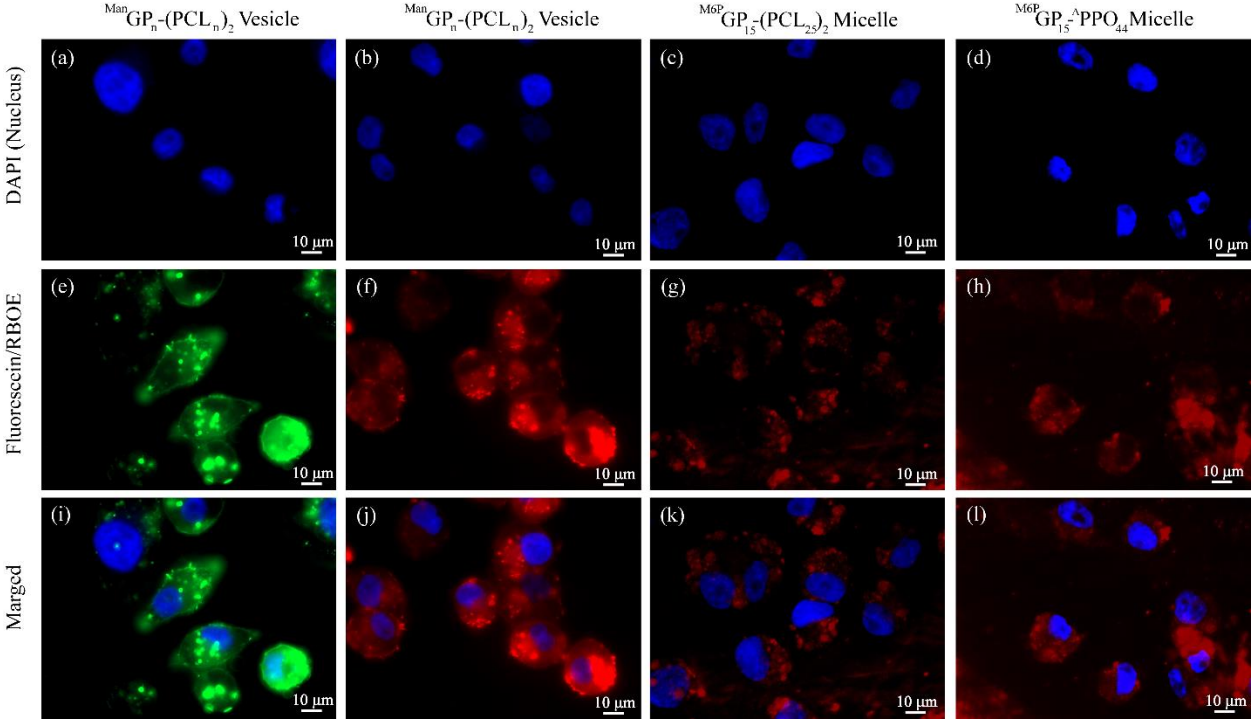

Figure S18 Epifluorescence microscopy imaging of Calcein-Loaded $^{Man}GP_n$-$(PCL_n)_2$ vesicle (a, e and i); RBOE-Loaded $^{Man}GP_n$-$(PCL_n)_2$ vesicle (b, f and j); RBOE-Loaded $^{M6P}GP_{15}$-$(PCL_{25})_2$ micelle (c, g and k) and RBOE-Loaded $^{M6P}GP_{15}$-$^{A}PPO_{44}$ micelle (d, h and l).

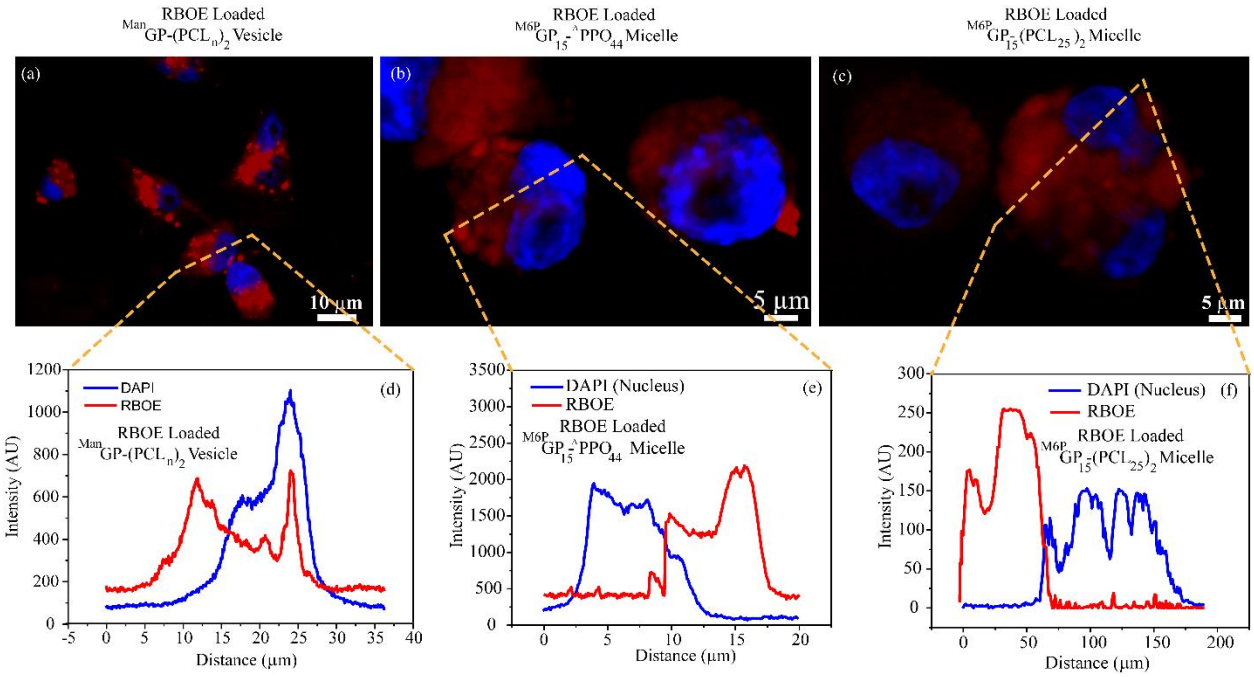

Figure S19 Epifluorescence microscopy imaging and corresponding color intensity profile of RBOE-Loaded $^{Man}GP_n$-$(PCL_n)_2$ vesicle (a and d); RBOE-Loaded $^{M6P}GP_{15}$-$^{A}PPO_{44}$ micelle (b and e) and RBOE-Loaded $^{M6P}GP_{15}$-$(PCL_{25})_2$ micelle (c and f).

Discussion: The color intensity profile from the bright area of the merged images ($^{M6P}GP_{15}$-$^{A}PPO_{44}$ and $^{M6P}GP_{15}$-$(PCL_{25})_2$) displays the variation of color intensity with distance for both the blue and red detection channels, which further supports the hypothesis that the dye, RBOE is internalized in Lysosome specifically. Whereas the color intensity profile of ^{Man}GP-$(PCL_n)_2$ indicated that the dye is internalized in lysosome and nucleus (no specificity). These experiments demonstrate that the uptake of RBOE loaded

^{M6P}GP based nanocarrier by MDA-MB-231 specifically trafficked to the lysosomal compartments.

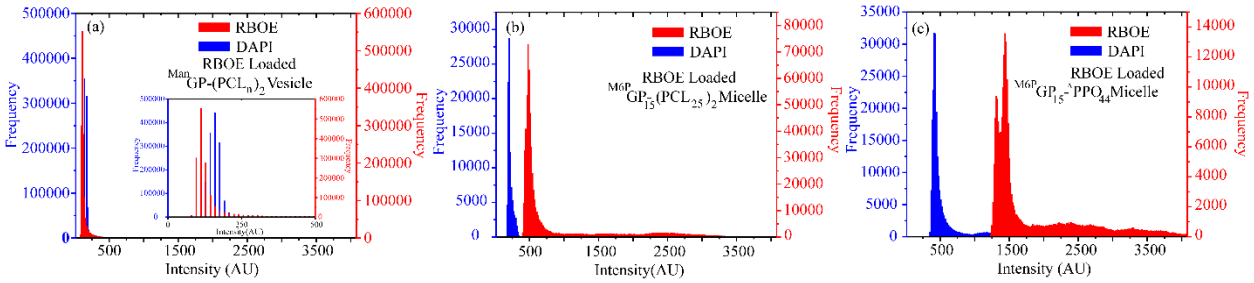

Figure S20 Histogram profile of RBOE-Loaded $^{Man}GP_n$-$(PCL_n)_2$ vesicle (a); RBOE-Loaded $^{M6P}GP_{15}$-$(PCL_{25})_2$ micelle (b) and RBOE-Loaded $^{M6P}GP_{15}$-$^{A}PPO_{44}$ micelle (c).

Discussion: From histogram profile, it was observed that the uptake intensity for ^{M6P}GP based nanocarrier is significantly higher as compared to ^{Man}GP based nanocarriers, which supports clathrin-mediated endocytosis (CME) data.

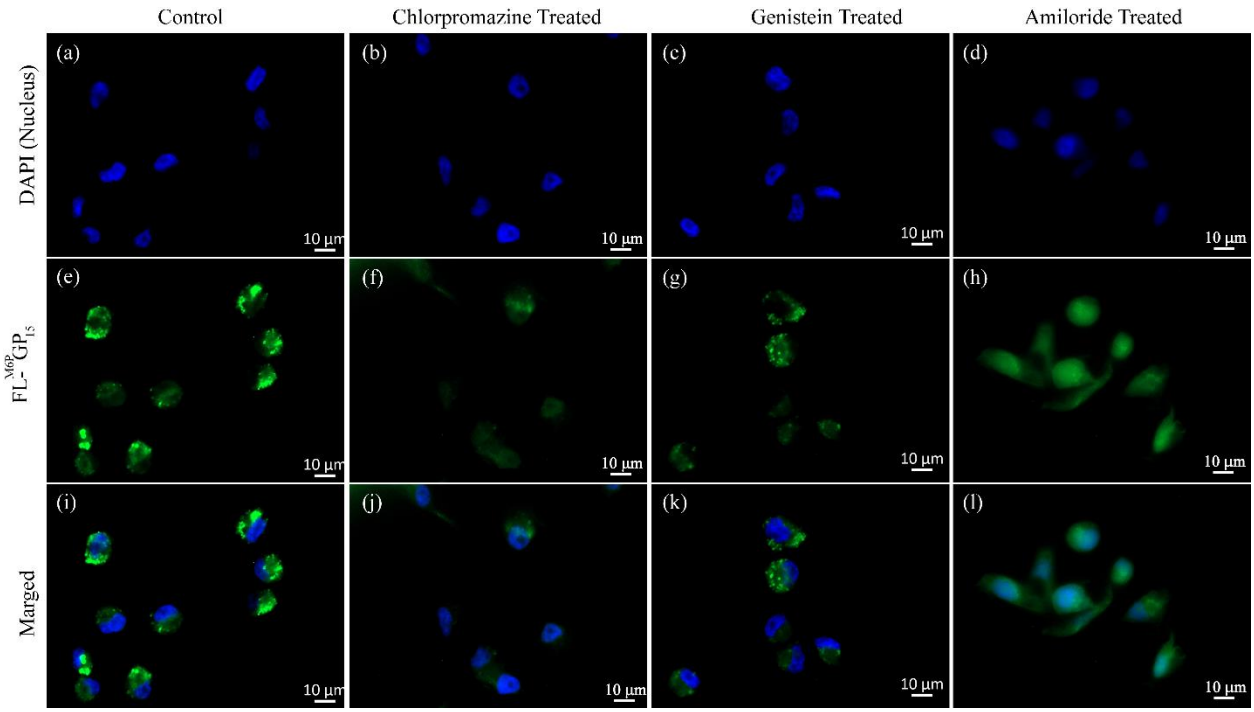

Figure S21 Epifluorescence microscopy imaging of FL-$^{M6P}GP_{15}$ polymer: Without any inhibitor (a, e, and i); Chlorpromazine treated (b, f, and j); Genistein treated (c, g, and k); Amiloride treated (d, h and l).

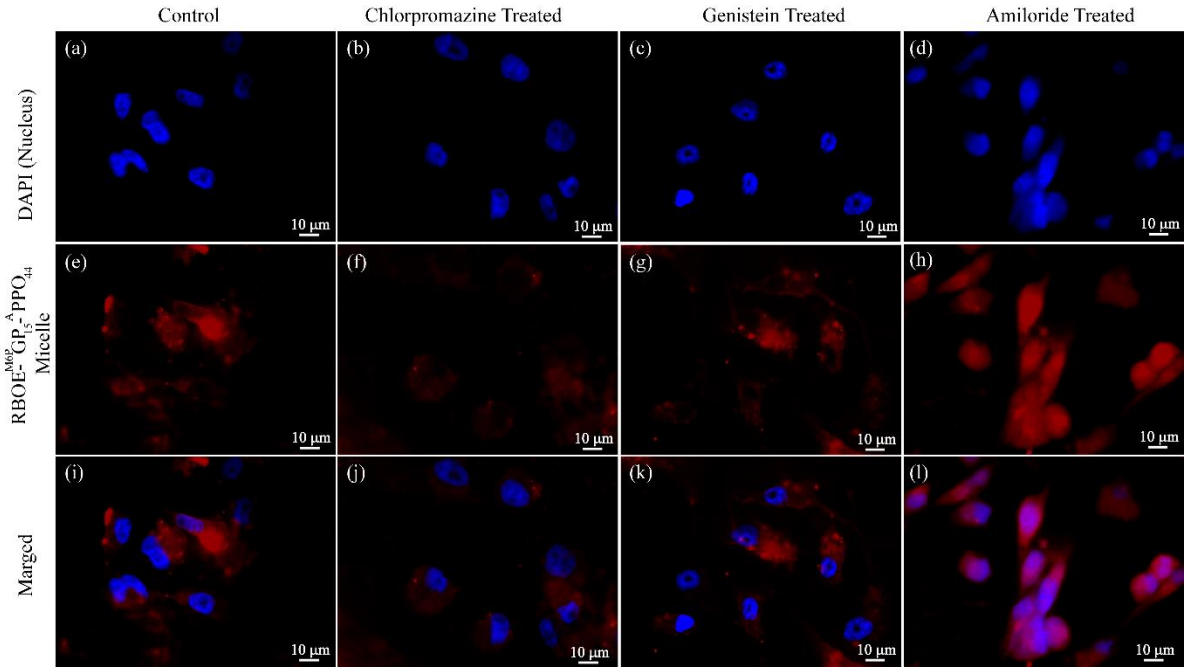

Figure S22 Epifluorescence microscopy imaging of RBOE-Loaded $^{M6P}GP_{15}$-$^{A}PPO_{44}$ micelle: Without any inhibitor (a, e, and i); Chlorpromazine treated (b, f, and j); Genistein treated (c, g, and k); Amiloride treated (d, h, and l).

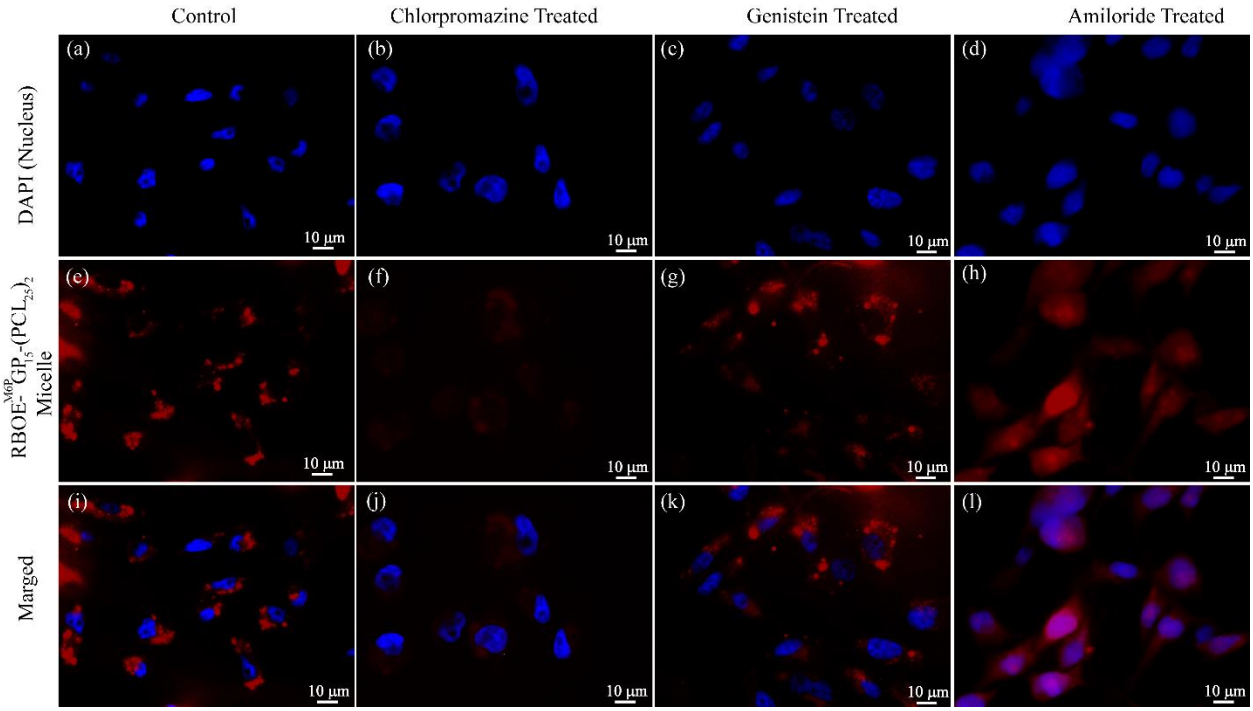

Figure S23 Epifluorescence microscopy imaging of RBOE-Loa0jded $^{M6P}GP_{15}$-$(PCL_{25})_2$ micelle: Without any inhibitor (a, e, and i); Chlorpromazine treated (b, f, and j); Genistein treated (c, g, and k); Amiloride treated (d, h, and l).

Note: For the above three experiments (Figure S15, S16, and S17) Chlorpromazine, Amiloride and genistein experiment was carried out for 30 minutes polymer uptake, 30 minutes pretreatment with drug and in complete media with 10% FBS at all times. Here there were two-time drug addition, one at the time of pre-incubation and after this media was removed, and then complete fresh media with drug and polymer were added for uptake study.

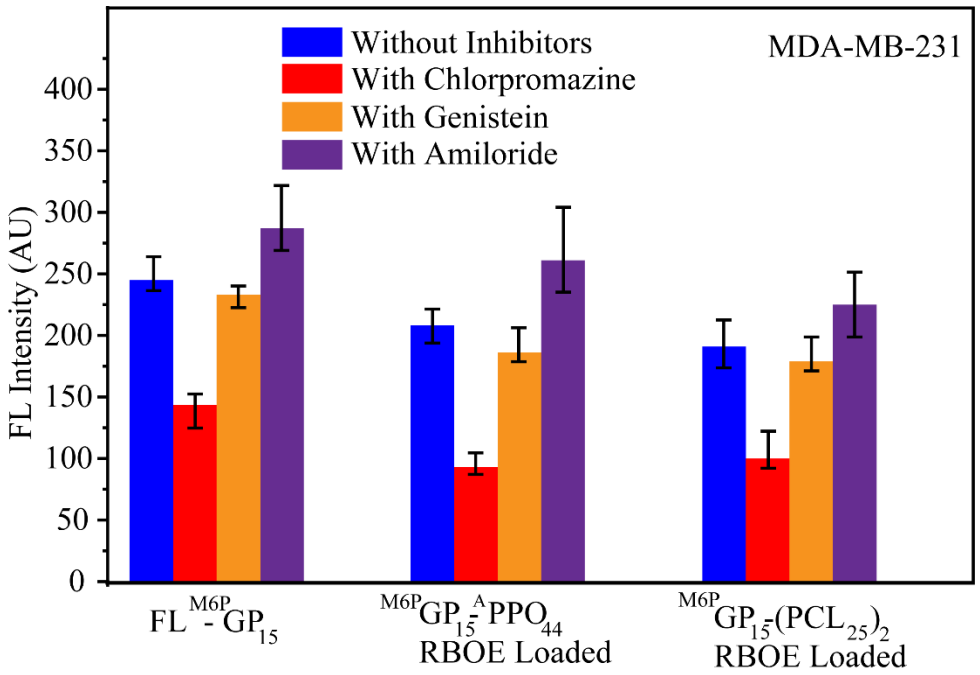

Figure S24. Intensity of epifluorescence microscopy image of FL-$^{M6P}GP_{15}$, RBOE loaded $^{M6P}GP_{15}$-$^{A}PPO_{44}$ nanocarrier and RBOE loaded $^{M6P}GP_{15}$-$(PCL_{25})_2$ nanocarrier in the presence and absence of inhibitors chlorpromazine, amiloride and genistein.

Table S1 Molecular weight distribution of polymers (GPC and NMR)

Polypeptide	**M_n (Theoretical) Da**	**M_n (NMR) Da**	**M_w (GPC) Da**	**PDI (GPC)**
$^{M6P}GP_{15}$	10,800	9,750	11,375	1.20
$^{M6P}GP_{15}$-$(PCL)_2$	16,500	17,895	17,325	1.25
$^{M6P}GP_{15}$-ace-PPO	13,300	13,785	12,935	1.23

Table S2 Statistically analysed “p” value with one-way ANOVA by using PAST software

Sample	'p' value
Transferrin (w/o chlorpromazine)	$5.13E^{-05}$
$^{M6P}GP_{15}$ (w/o chlorpromazine)	$8.37E^{-08}$
$^{M6P}GP_{15}$-$(PCL_{25})_2$ (w/o chlorpromazine)	0.004154
$^{M6P}GP_{15}$-$^{A}PPO_{44}$ (w/o chlorpromazine)	$1.50E^{-06}$

^{1}H NMR, and ^{31}P Spectra of the compounds

(* peak in NMR indicates residual solvents peak)

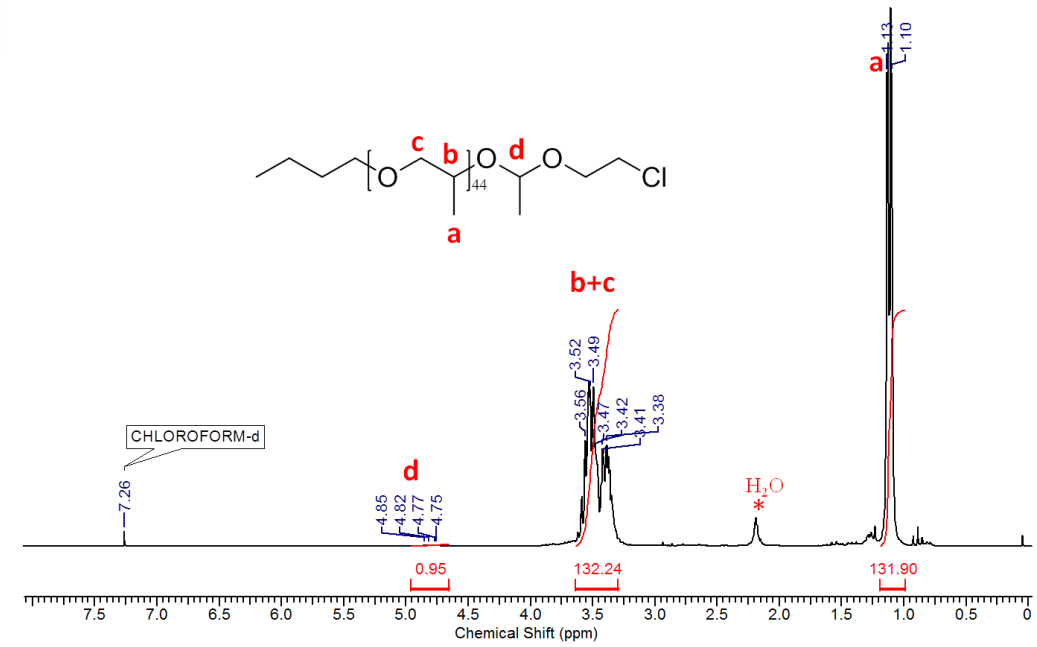

Figure S25 ^{1}H NMR ($CDCl_3$, 200 MHz) Spectrum of Cl-$^{A}PPO_{44}$ polymer

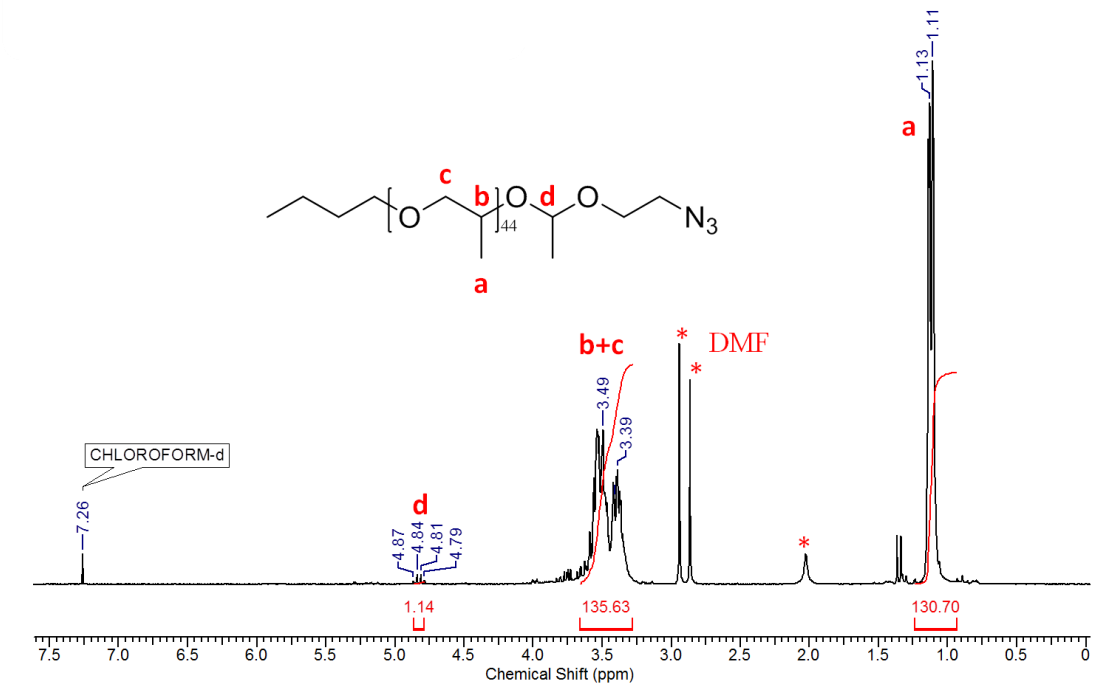

Figure S26 ^{1}H NMR ($CDCl_3$**,** 200 MHz) Spectrum of N_3-$^{A}PPO_{44}$ polymer

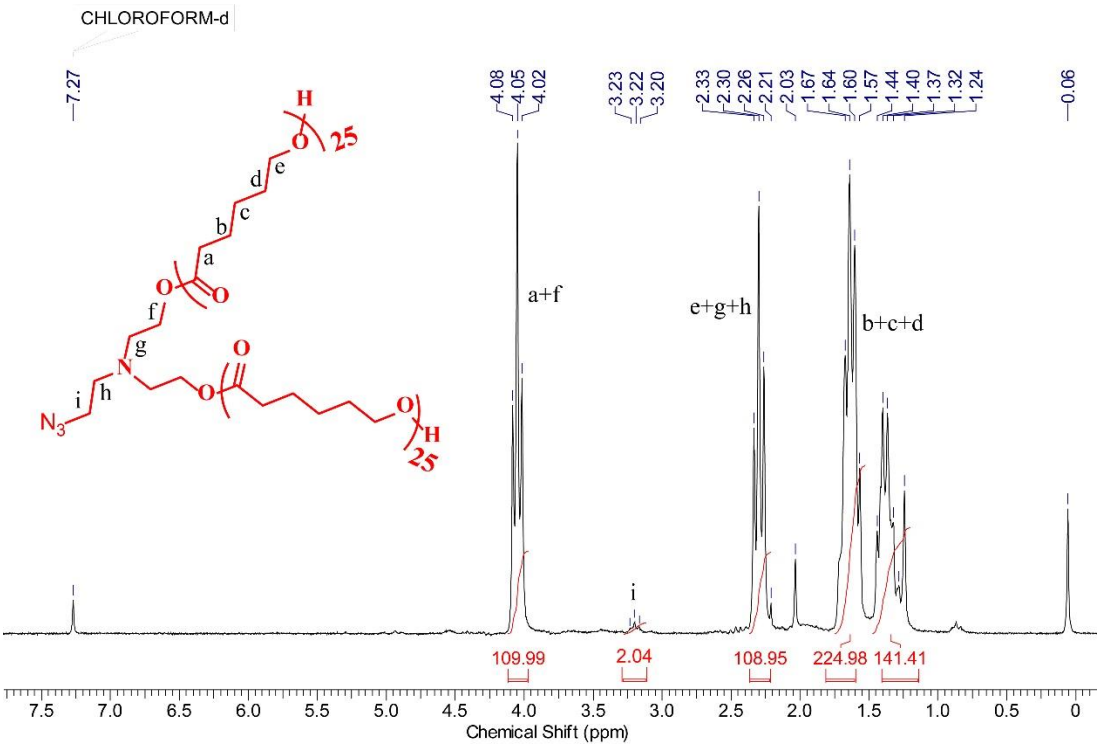

Figure S27 ^{1}H NMR ($CDCl_3$, 200 MHz) Spectrum of N_3-$(PCL_{25})_2$ polymer

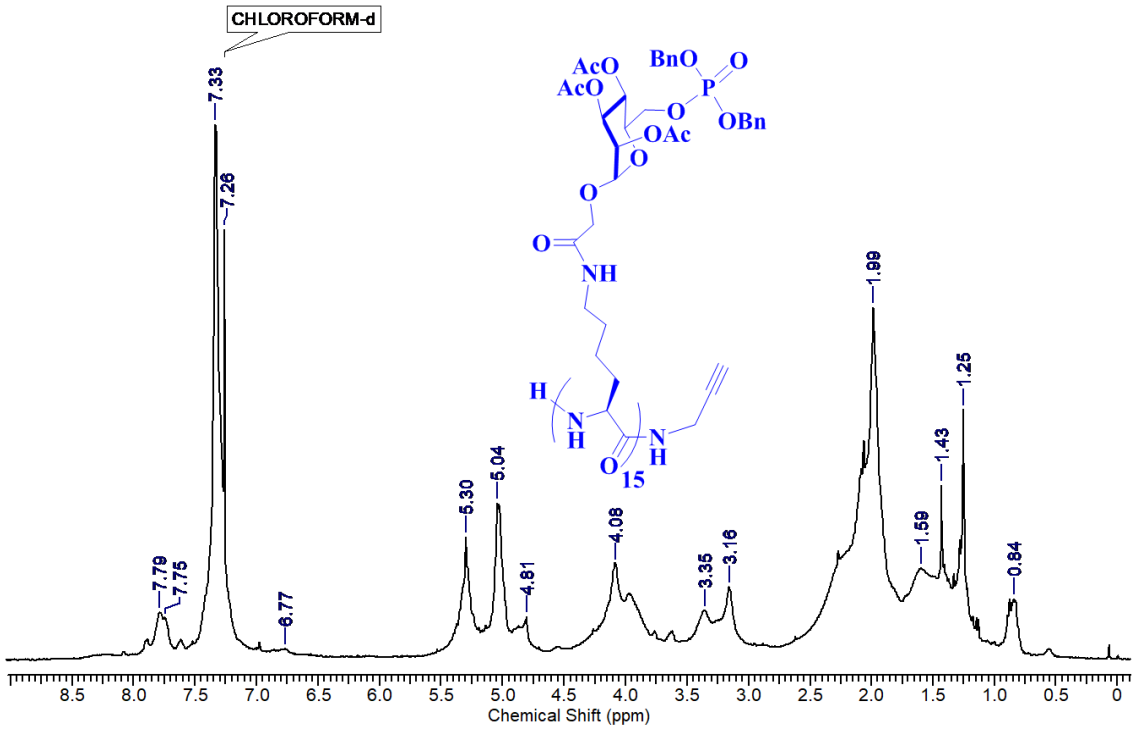

Figure S28 ^{1}H NMR ($CDCl_3$, 400 MHz) Spectrum of Pr-^{M6P}AcGP_{15} polymer

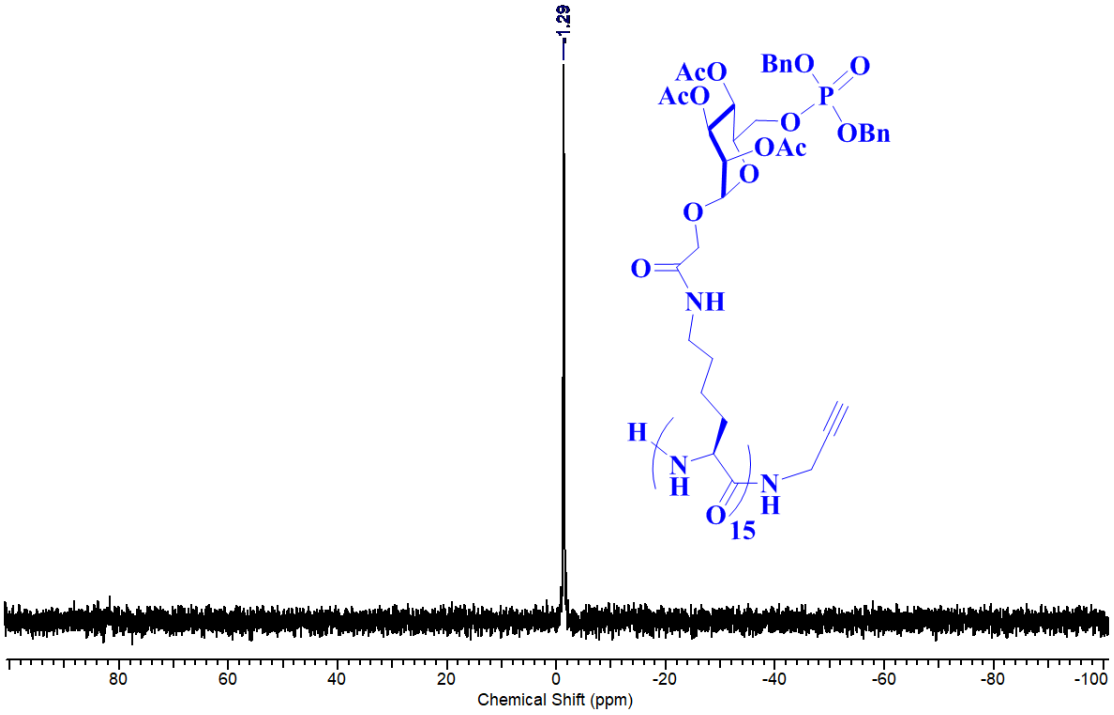

Figure S29 ^{31}P NMR ($CDCl_3$, 202.46 MHz) Spectrum of Pr-$^{M6P}AcGP_{15}$

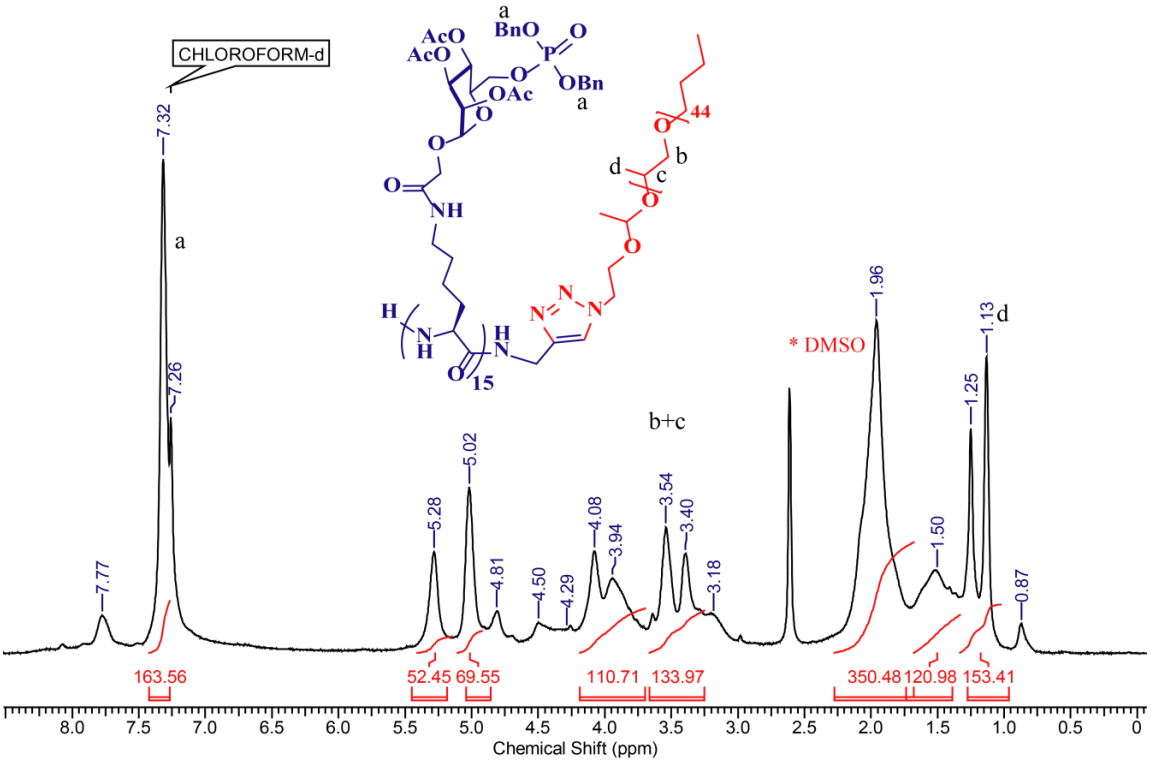

Figure S30 ^{1}H NMR ($CDCl_3$, 400 MHz) Spectrum of $^{M6P}AcGP_{15}$-$^{A}PPO_{44}$ block copolymer

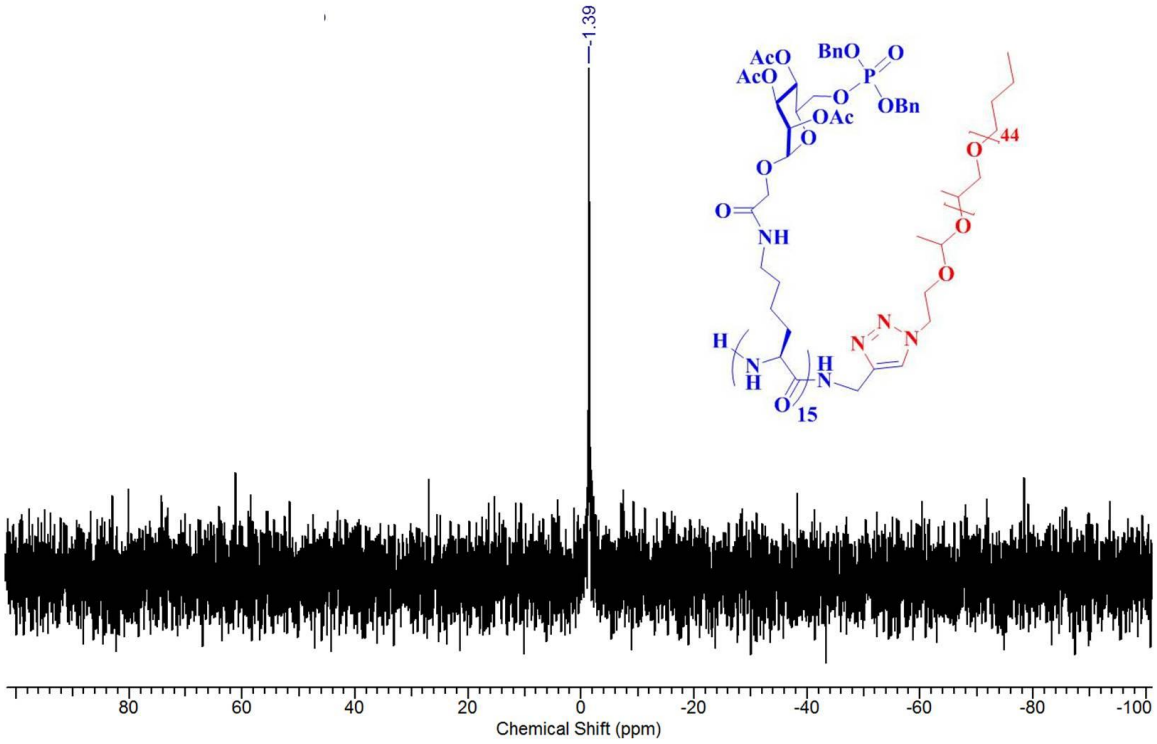

Figure S31 ^{31}P NMR ($CDCl_3$, 202.46 MHz) Spectrum of $^{M6P}AcGP_{15}$-$^{A}PPO_{44}$ block copolymer

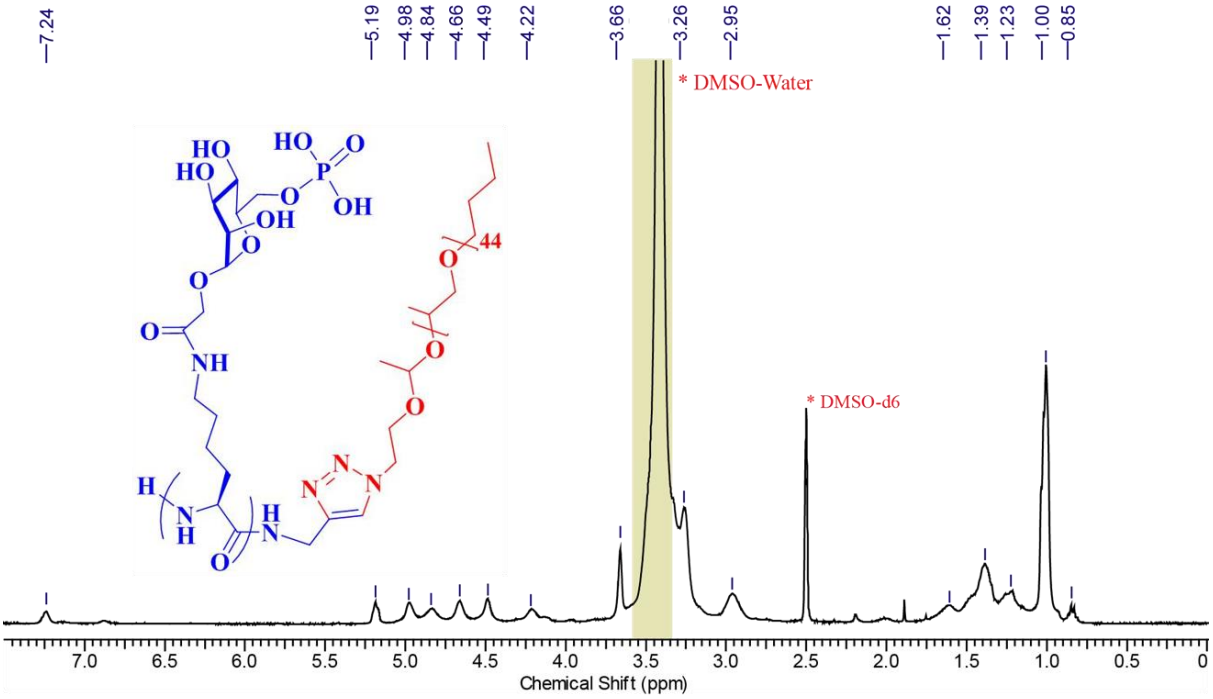

Figure S32 ^{1}H NMR (DMSO-d_6, 400 MHz) Spectrum of $^{M6P}GP_{15}$-$^{A}PPO_{44}$ block copolymer

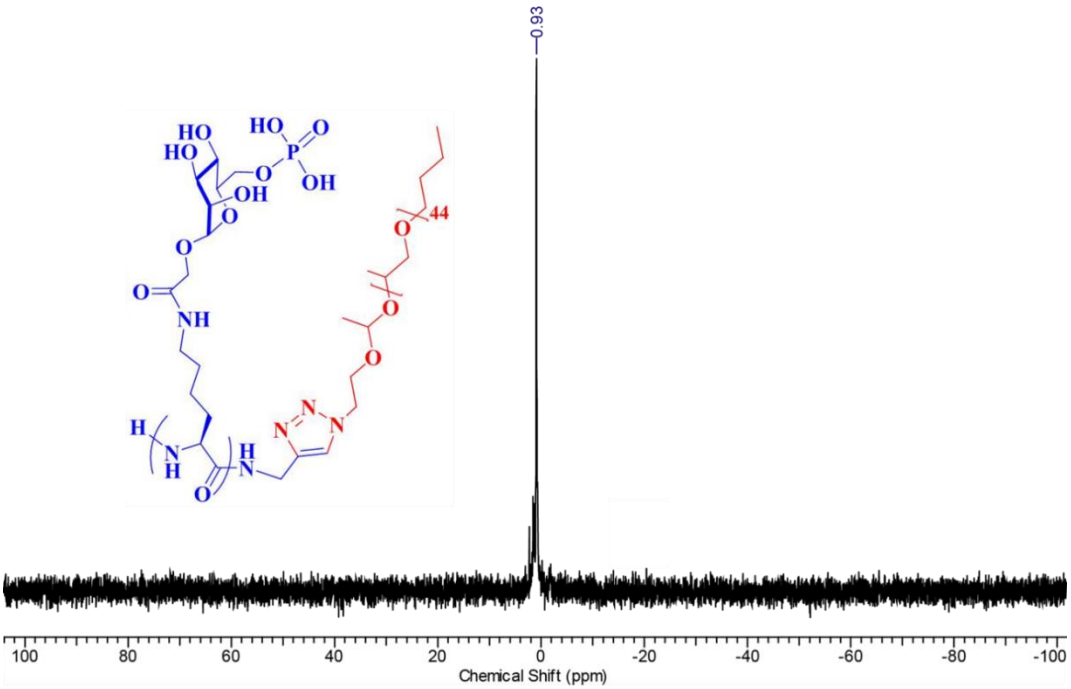

Figure S33 ^{31}P NMR (DMSO-d_6, 202.46 MHz) Spectrum of $^{M6P}GP_{15}$-$^{A}PPO_{44}$ block copolymer

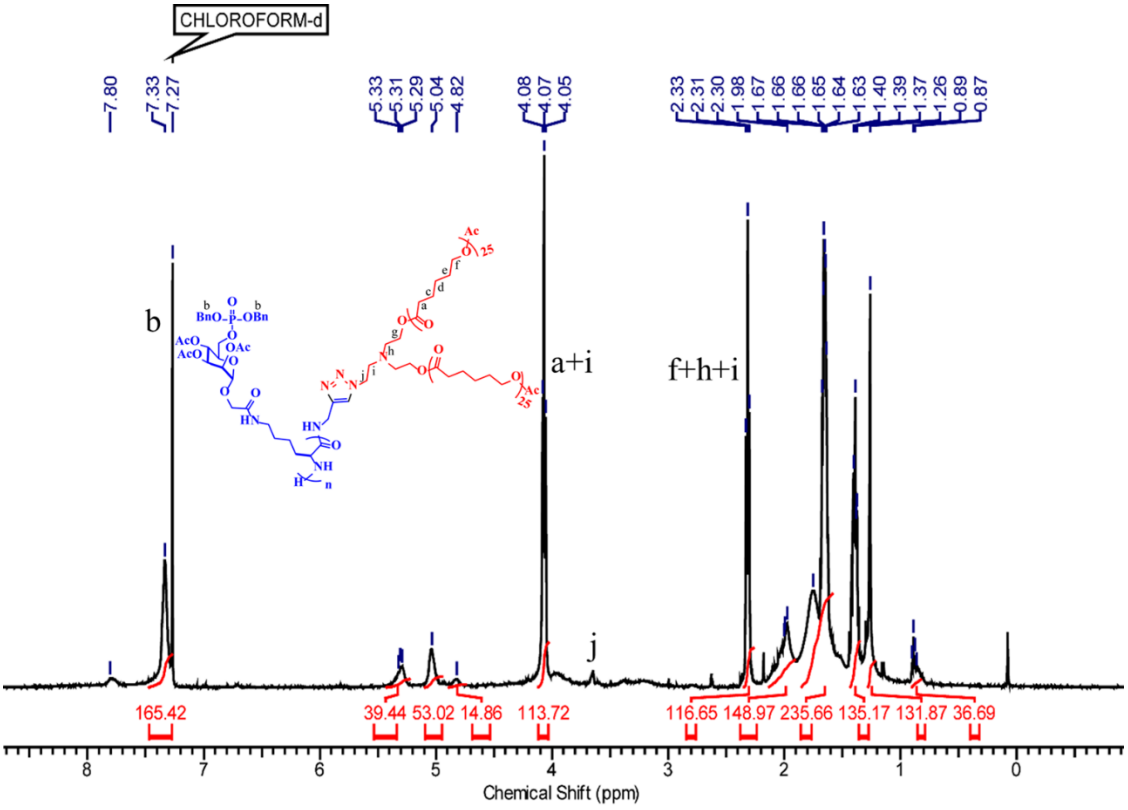

Figure S34 ^{1}H NMR ($CDCl_3$, 400 MHz) Spectrum of $^{M6P}AcGP_{15}$-$(PCL_{25})_2$ block copolymer

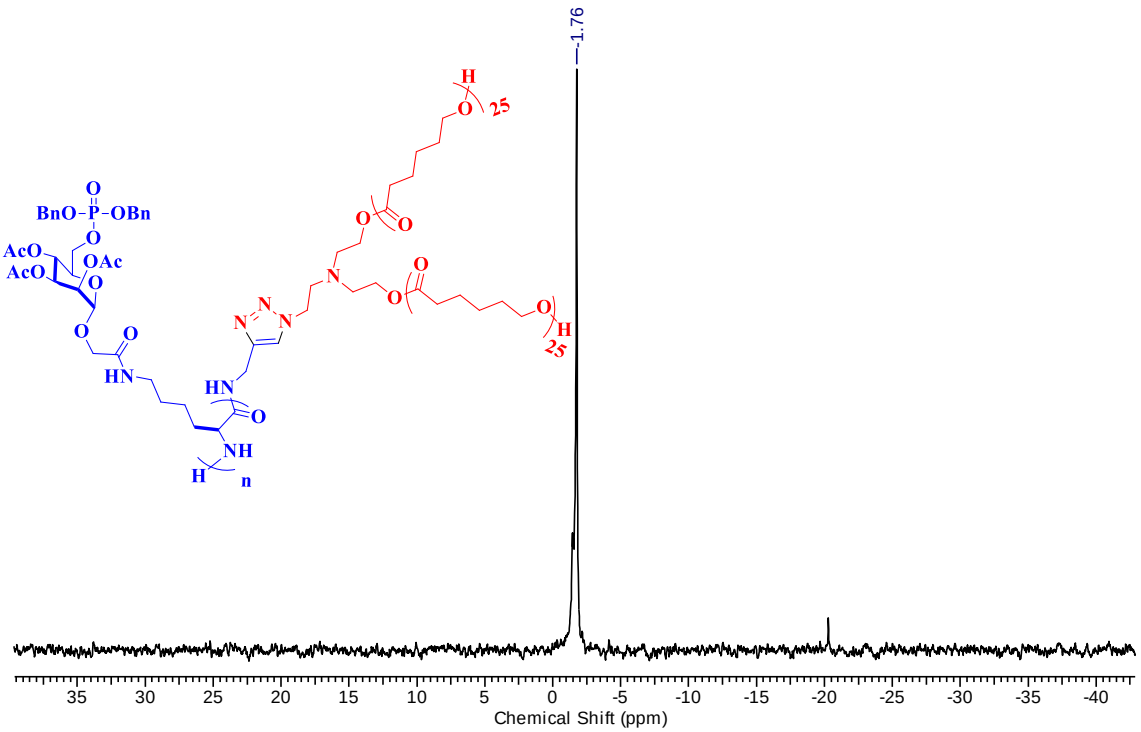

Figure S35 ^{31}P NMR ($CDCl_3$, 202.46 MHz) Spectrum of $^{M6P}AcGP_{15}$-$(PCL_{25})_2$ block copolymer

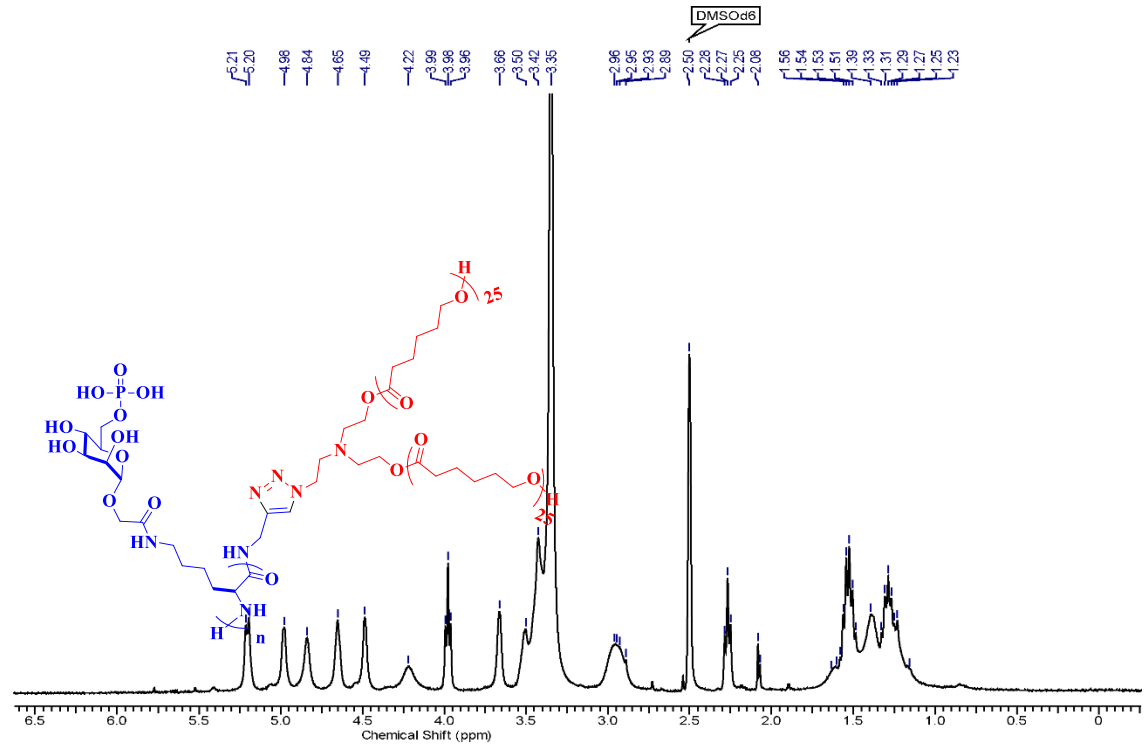

Figure S36 ^{1}H NMR (DMSO-d_6, 400 MHz) Spectrum of $^{M6P}AcGP_{15}$-$(PCL_{25})_2$ block copolymer

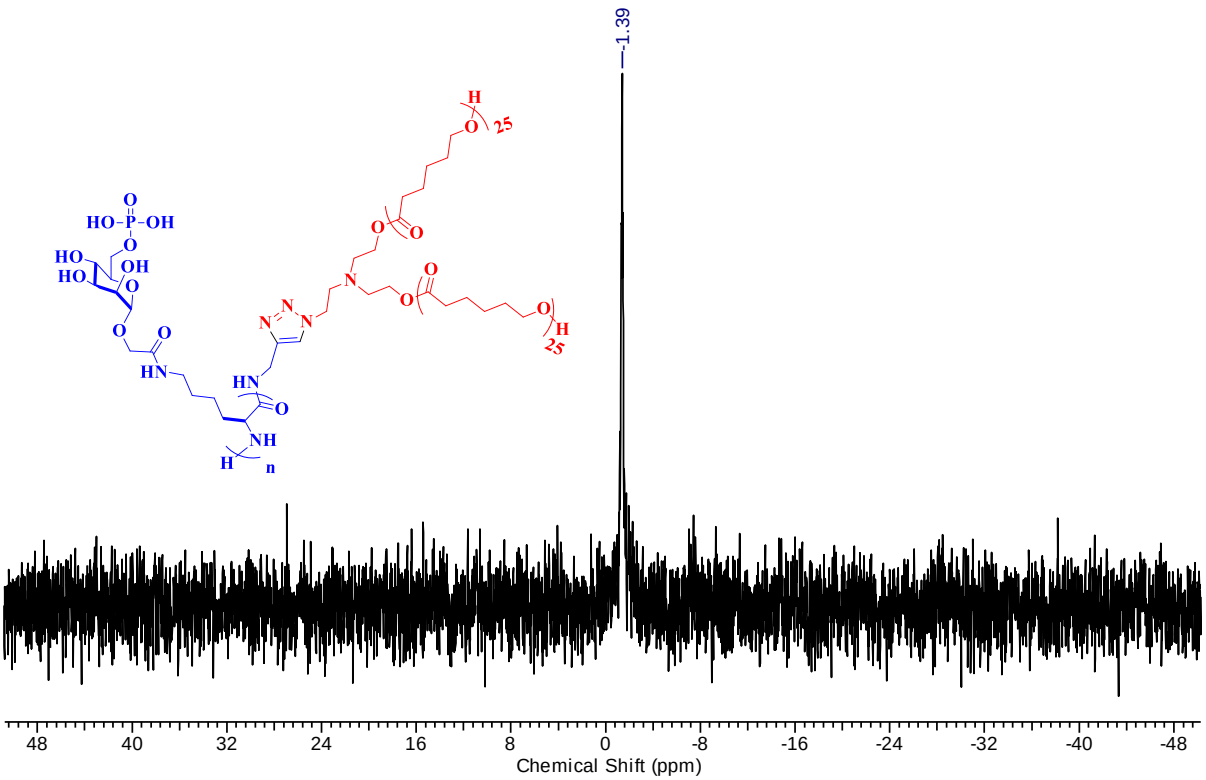

Figure S37 ^{31}P NMR (DMSO-d_6, 202.46 MHz) Spectrum of $^{M6P}AcGP_{15}$-$(PCL_{25})_2$ block copolymer